Phytochemical analysis, *in-vitro* and *in-silico* study of antiproliferative activity of ethyl acetate fraction of *Launaea cornuta* (Hochst. ex Oliv. & Hiern) C. Jeffrey against human cervical cancer cell line

Inyani John Lino Lagu[1]*, Dorothy Wavinya Nyamai[2] and Sospeter Ngoci Njeru[3]*

[1]Department of Molecular Biology and Biotechnology, Pan African University Institute for Basic Sciences, Technology and Innovation, Nairobi, Kenya, [2]Department of Biochemistry, School of Biomedical Sciences, College of Health Sciences, Jomo Kenyatta University of Agriculture and Technology, Nairobi, Kenya, [3]Centre for Traditional Medicine and Drug Research (CTMDR), Kenya Medical Institute (KEMRI), Nairobi, Kenya

Introduction: Cervical cancer is one of the leading causes of death among women globally due to the limitation of current treatment methods and their associated adverse side effects. *Launaea cornuta* is used as traditional medicine for the treatment of a variety of diseases including cancer. However, there is no scientific validation on the antiproliferative activity of *L. cornuta* against cervical cancer.

Objective: This study aimed to evaluate the selective antiproliferative, cytotoxic and antimigratory effects. *L. cornuta* and to explore its therapeutical mechanisms in human cervical cancer cell lines (HeLa-229) through a network analysis approach.

Materials and methods: The cytotoxic effect of *L. cornuta* ethyl acetate fraction on the proliferation of cervical cancer cells was evaluated by 3-(4, 5-dimethylthiazol-2-yl)-2, 5-diphenyltetrazolium bromide (MTT) bioassay and the antimigratory effect was assessed by wound healing assays. Compounds were analysed using the qualitative colour method and gas chromatography-mass spectroscopy (GC-MS). Subsequently, bioinformatic analyses, including the protein-protein interaction (PPI) network analysis, Gene Ontology (GO), and Kyoto Encyclopaedia of Genes and Genomes (KEGG) analysis, were performed to screen for potential anticervical cancer therapeutic target genes of *L. cornuta.* Molecular docking (MD) was performed to predict and understand the molecular interactions of the ligands against cervical cancer. Reverse transcription-quantitative polymerase chain reaction (RT-qPCR) was performed to validate the network analysis results.

Results: *L. cornuta* ethyl acetate fraction exhibited a remarkable cytotoxic effect on HeLa-229 proliferation (IC_{50} of 20.56 ± 2.83 μg/mL) with a selectivity index (SI) of 2.36 with minimal cytotoxicity on non-cancerous cells (Vero-CCL 81 (IC_{50} of

48.83 ± 23.02). The preliminary screening revealed the presence of glycosides, phenols, saponins, terpenoids, quinones, and tannins. Thirteen compounds were also identified by GC-MS analysis. 124 potential target genes associated with the effect of *L. cornuta* ethyl acetate fraction on human cervical cancer were obtained, including AKT1, MDM2, CDK2, MCL1 and MTOR were identified among the top hub genes and PI3K/Akt1, Ras/MAPK, FoxO and EGFR signalling pathways were identified as the significantly enriched pathways. Molecular docking results showed that stigmasteryl methyl ether had a good binding affinity against CDK2, ATK1, BCL2, MDM2, and Casp9, with binding energy ranging from −7.0 to −12.6 kcal/mol. Tremulone showed a good binding affinity against TP53 and P21 with −7.0 and −8.0 kcal/mol, respectively. This suggests a stable molecular interaction of the ethyl acetate fraction of *L. cornuta* compounds with the selected target genes for cervical cancer. Furthermore, RT-qPCR analysis revealed that CDK2, MDM2 and BCL2 were downregulated, and Casp9 and P21 were upregulated in HeLa-229 cells treated with *L. cornuta* compared to the negative control (DMSO 0.2%).

Conclusion: The findings indicate that *L. cornuta* ethyl acetate fraction phytochemicals modulates various molecular targets and pathways to exhibit selective antiproliferative and cytotoxic effects against HeLa-229 cells. This study lays a foundation for further research to develop innovative clinical anticervical cancer agents.

Introduction

Cervical cancer is a major global health disease that affects women (Drokow et al., 2022). It is one of the leading causes of cancer death among women and the fourth most common cancer worldwide (Revathidevi et al., 2021). Human papillomavirus is the primary aetiological driver in carcinogenesis (Balasubramaniam et al., 2019). Not all human papillomavirus (HPV) infections in women result in cervical cancer. High-risk HPV genotypes induce a normal cell to transform into a precancerous lesion, which subsequently becomes an invasive lesion (Kasi et al., 2021). HPV infection causes the overexpression of viral oncogenes, which may inhibit a number of cellular proteins and affect biological processes such as cell proliferation, cell cycle, and apoptosis (Martínez-Rodríguez et al., 2021).

Globally, in 2020, a total of 604127 cases of cervical cancer were estimated, and 341831 deaths were recorded (Olthof et al., 2024). The incidence rate was 13.3 cases per 100,000 women, and the mortality rate was 7.2 deaths per 100,000 women (Singh et al., 2023). Over 58% of cervical cancer cases globally were estimated in Asia, followed by Africa (20%), Europe (10%) and Latin America (10%) (Singh et al., 2023). However, the incidence and mortality rates for cervical cancer are exceptionally high in Sub-Saharan Africa at 19.59% and 24.55% annual global burden, respectively (Black and Richmond, 2018).

Botanicals' secondary metabolites and their derivatives have been evaluated in oncology-related clinical research and trials (Omara et al., 2022). The comprehensive knowledge on the mechanism of action for some investigated plant compounds provided the basis to develop novel, efficacious, safer botanical-derived compounds or their semi-synthetic analogues. Such had additional therapeutic advantages over the convectional chemotherapeutic drugs, which are associated with high toxicity not only to cancer cells but also to noncancerous cells (Scatchard et al., 2012; Vordermark, 2016; Johnson et al., 2018; Paken et al., 2023). Cervical cancer has become resistant to conventional therapeutic drugs, including cisplatin, paclitaxel, and carboplatin (Small et al., 2017), thus rendering them less effective. Hence, it was imperative to speed up research on botanical plants as an alternative source of less toxic, more tolerable and effective anticancer drugs for cervical cancer treatment.

The rich biodiversity has contributed significantly to traditional medicine and medicinal systems since ancient times (Omara, 2020). Approximately 1,200 medicinal plants are used in Kenya, 41 of which have anticancer properties, which account for only 10% of the medicinal plants (Onyancha et al., 2018). Botanical-based drugs are gaining attention due to their low toxicity, availability, cost-effectiveness, and tolerability compared to conventional drugs (Tariq et al., 2017; Ochwang'i et al., 2014; Misonge et al., 2016). In this study, *Launaea cornuta* (Hochst. ex Oliv. & Hiern) C. Jeffrey also known as "mchunga" was investigated. *L. cornuta* is an erect herbaceous perennial plant belonging to the Asteraceae family, characterised by a hollow leafy and stem, slightly succulent, glabrous, with milky juice and grows to a height of about 1.5 m (J et al., 2015). It is indigenous to Kenya, Burundi, Cameroon, Uganda, Nigeria, Rwanda, Chad, Djibouti, Eritrea, Ethiopia, Malawi, Mozambique, Somalia, Sudan, Tanzania, Zambia, Central African Republic, Zaïre, and Zimbabwe (Machocho et al., 2014; Omara et al., 2022). In Kenyan communities, this plant is used as a wild vegetable

and a source of vitamin C (Musila et al., 2013). The localised budding root concoction known as 'Kipche' is used to cure throat cancer ("Koroitab mokto"), typhoid, gonorrhoea, benign prostate hyperplasia, and breast cancer, among others (J et al., 2015; Fatuma Some, 2014; Khan et al., 2016; Chemweno et al., 2022). Regardless of the extensive use of *L. cornuta* plants in traditional medicine, their therapeutic efficacy, and toxicity have not been empirically validated, especially in cervical cancer.

In this study, we systemically evaluated the anticancer activity of the ethyl acetate fraction of *L. cornuta*, analysed and identified compounds using the GC-MS approach and explored the relevant targets and pathways involved in eliciting the anticervical effects through a network analysis approach.

Materials and methods

Samples collection and extract preparation

Fresh stems and leaves of *L. cornuta* (Hochst. ex Oliv. & Hiern) C. Jeffrey were collected from Embu County, Mbeere South sub-County, Mavuria ward (Latitude 0°46′27.0″S 37°40′54.9″E and Longitude −0.774156, 37.681908). The plant was not classified as an endangered species, and therefore, no prior permission/consent was sought during the plant material collection phase. Plant identification and authentication were performed by a botanist at the University of Nairobi, and a voucher specimen number NSN18 was given and deposited at the Kenyan National Museums - Eastern Africa Herbarium. The stems and leaves were washed under running tap water, dried under a shade for 3 weeks and milled into a fine powder using an electric grinder (Christy 8 MILL, serial No; 51474). The plant powder was extracted using dichloromethane: methanol solvent following a method described by Okpako et al., with some modifications to obtain the crude extract (Okpako et al., 2023a) and three fractions: n-hexane, ethyl acetate, and water were obtained. The crude extract obtained was macerated in 250 mL of n-hexane solvent, shaken vigorously and left undisturbed for about 20 min. Thereafter, the hexane fraction was separated. Another 250 mL was added to the residues from the first fractionation, and the process was repeated after the two hexane fractions were pooled together. The resulting residues were further fractionated with water and ethyl acetate solvents. The resulting mixtures with intermittent shaking for 30 min were left to stand for 24h and were separated based on the solvent interphase. The organic solvent fractions were concentrated with a rotor evaporator, as described before (Okpako et al., 2023a). The crude extract and the fraction of hexane, water and ethyl acetate were stored at −20°C until analysis.

Cell lines and culture conditions

A human cervical cancer cell line (HeLa-229) and a kidney epithelial cell line derived from the African green monkey (Vero-CCL) were purchased from ATCC and cultured in Essential Modified Eagle Medium (EMEM) supplemented with 1% L-glutamine (200 mM), 10% fetal bovine serum (FBS), 1.5% sodium bicarbonate, 1% HEPES (1M), 1% penicillin-streptomycin and 0.25 μg/mL amphotericin B. The cell culture was conducted at 37°C under a humidified atmosphere and 5% CO_2 to achieve 75% – 80% confluence.

Antiproliferative and cytotoxicity assay

The effects of *L. cornuta* fractions and crude extract on the proliferation of HeLa cells were evaluated using the 3-(4, 5-dimethylthiazol-2-yl)-2, 5-diphenyltetrazolium bromide (MTT) assay (Solarbio, China) following a method described by Nyeru *et al.* and Sergazy *et al.* with some modification (Njeru and Muema, 2021; Sergazy et al., 2021). The HeLa-229 cells (1.0 × 10^4 cells/mL) were seeded in a 96-well plate containing fresh EMEM medium and incubated for 24 h. Subsequently, the medium was aspirated, and 100 μL of 200 μg/mL of the plant fractions and the total extract were added and incubated for 48 h. Doxorubicin (200 μg/mL) was used as a positive control, and 0.2% dimethyl sulfoxide was used as a negative control. After incubation for 48 h, 10 μL of freshly prepared 5 μg/mL MTT was added to each well and incubated for 4 h. MTT was then aspirated, and 100 μL of 100% dimethyl sulfoxide (DMSO, Finar Chemicals, India) was added to dissolve formazan crystals. The absorbance was read at 570 and 720 nm using a plate reader (Infinite M1000 by Tecan). All experiments were carried out in four replicates, and the percentage cell viability was calculated using the formula presented below (Juwitaningsih et al., 2022).

$$\text{Cell viability (\%)} = [\,(\text{Absorbance of treated cell} - \text{Absorbance of culture medium})/(\text{Absorbance of untreated cell} - \text{Absorbance of culture medium}) \times 100\,]$$

The *L. cornuta* ethyl acetate fraction, which gave less than 50% cell viability after 48 h of incubation, was considered to have anti-cervical cancer activity and was prioritised for further downstream investigations. Thereby, ethyl acetate fraction was selected for dose-dependent tests using a range of concentrations (2.0–64.0 μg/mL) and (4.0–256 μg/mL) for the cytotoxic effect on HeLa-229 and Vero-CCL cells, respectively. The half-maximal inhibitory concentration (IC_{50}) and the half-maximal cytotoxicity concentration (CC_{50}) were determined using dose-response and dose-cytotoxicity graphs and calculated by a non-linear regression method using GraphPad Prism 8.4 (Panyajai et al., 2024). The selectivity index (SI) was calculated using the formula below (Mongalo et al., 2017).

$$\text{Selectivity Index (SI)} = [\,(CC_{50}\ \text{in μg/mL})/(IC_{50}\ \text{in μg/mL})\,]$$

Cell morphological study

To investigate the effects of *L. cornuta* ethyl acetate on HeLa 229 cells, the cells were treated with five different concentrations of the extract (4, 8, 16, 32, and 64 μg/mL) for a period of 48 h. The morphological changes in HeLa cells were then determined with a digital microscope at ×20 magnification.

Wound healing assay

HeLa 229 cells were cultured in a 6-well plate at a density of 1×10^6 cells/mL per well and incubated for 24 h to form a monolayer. A wound was created using a sterile 200 mL pipette tip. The cells were then treated with *L. cornuta* ethyl acetate fraction at the concentration corresponding to the IC_{50} (20.56 μg/mL) and incubated for 48 h. During the treatment period, cells were imaged using a digital microscope at 0 h, 24 h and 48 h. The distance between the wounds on the cells was measured and analysed with ImageJ software. The relative migration distance was calculated and expressed as a percentage, as shown below.

Relative migration distance (%) = [(Distance within the scratch at 0 h – Distance within the scratch at 24 h)/ (Distance within the scratch at 0 h) x 100]

Preliminary screening and phytochemical analysis using GC-MS

We performed a preliminary screening for the presence of alkaloids, glycosides phenols, flavonoids, terpenoids, steroids, quinones, saponins, and tannins in *L. cornuta* ethyl acetate fraction, which exhibited anti-cancer activity using methods described previously (Njeru et al., 2015; Yadav et al., 2017; Shaikh and Patil, 2020) and subsequently, gas chromatography-mass spectrometer system (Model; Shimadzu, GC-MS QP-2010SE) was used for quantitative analysis. The system was equipped with a low-polarity BPX5 capillary column (30 m × 0.25 mm × 0.25 μm film thickness). The oven temperature was set at 55°C for 1 min, then increased by 10°C per minute to reach a constant temperature of 280°C for 15 min and held for 30 s. The injector temperature was set at 200°C. Helium was used as the carrier gas with a 1.08 mL/min flow rate. The diluted sample (1% v/v) was injected (1 μL) into the GC with an AS3000 autosampler in a split ratio of 10:1. The mass detector was set at 200°C (ion source) and 250°C (interface temperature). Electron-ionisation mass spectra were collected at 70 eV in full scan mode at a m/z of 35–550. The identity of phytochemicals was determined by comparing the mass spectra with the spectra of compounds in the NIST library database (Wavinya Nyamai et al., 2015; Njeru and Muema, 2020).

Bioinformatics analysis

Drug likeness screening test

The PubChem CID and canonical SMILES (Simplified Molecular Input Line Entry System) of the GC-MS identified compounds of *L. cornuta* ethyl acetate were retrieved from PubChem (https://pubchem.ncbi.nlm.nih.gov/). The SMILES were then submitted to SwissADME and pkCSM tools (http://www.swissadme.ch/index.php & https://biosig.lab.uq.edu.au/pkcsm/prediction) to predict the druglike (DL), the pharmacokinetics and physiochemical properties of the compounds. The prediction was based on Lipinski's rule of five: blood-brain barrier (BBB), the central nervous system (CNS), human intestinal absorption, and inhibition of cytochrome P450s (Vishvakarma et al., 2023).

Identification of candidate targets for *Launaea cornuta* ethyl acetate fraction against human cervical cancer

The targets of the compounds were predicted from Swiss TargetPrediction (http://www.swisstargetprediction.ch/database), with 'humans' (*Homo sapiens*) as the study species with $p > 0.1$ considered potential targets (Daina et al., 2019). Additional targets were predicted using BindingDB (https://bindingdb.org/rwd/bind/chemsearch/marvin/FMCT.jsp), potential targets with $p > 0.7$ were considered and retrieved. The Gene IDs of the selected targets were retrieved from UniProtKB database (https://www.uniprot.org). Ensemble approach (SEA) (https://sea.bkslab.org/) database was used to predict the compound's targets based on the assumption that molecules with similar structures tend to have similar responses to a target (Wang et al., 2016). For each database, the term '*H. sapiens*' was used as the keyword. The results predicted from the three databases were pooled, and duplicates were removed (Li and Ren, 2022). The disease targets of human cervical cancer for development and progression were retrieved from GeneCards (https://www.genecards.org/), DisGeNET (https://www.disgenet.org/), OMIM (https://www.omim.org/) and Pharos (https://pharos.nih.gov/diseases/) databases using 'Cervical cancer' the disease type. All retrieved targets were merged, and only the unique targets were selected. Lastly, the potential targets of the identified compounds of *L. cornuta* ethyl acetate and the disease targets of cervical cancer were intersected using an online bioinformatics and evolutionary genomics platform (https://bioinformatics.psb.ugent.be/webtools/ven) to obtain the common target genes.

Protein-protein interaction (PPI) analysis

The STRING database (https://string-db.org/), version 12.0, was used to build a PPI network for the common target genes between the *L. cornuta* ethyl acetate fraction and cervical cancer targets. The species was set as "*H. sapiens*", and the interaction threshold was set to 0.4. Subsequently, the PPI data was exported as a 'TSV' format file and imported into Cytoscape software (version 3.10) for analysis. The Cytohubba plug-in in Cytoscape was used to determine and calculate the score (degree) of each node and the top 30 hub targets were selected (Zhang et al., 2021).

Gene ontology (GO) and Kyoto encyclopaedia of genes and genomes (KEGG) enrichment analyses

GO and KEGG pathway enrichment analysis was performed following the method described by Jeddi et al. with some modifications (Jeddi et al., 2023) for the common targets of between *L. cornuta* ethyl acetate fraction and cervical cancer using an online enrichment tool ShinyGO version 0.77 (https://ge-lab.org/go/), SRplot (Science and Research online plot (bioinformatics.com.cn) tool was used to identify the KEGG pathway and mapping associated with the targets, Human was
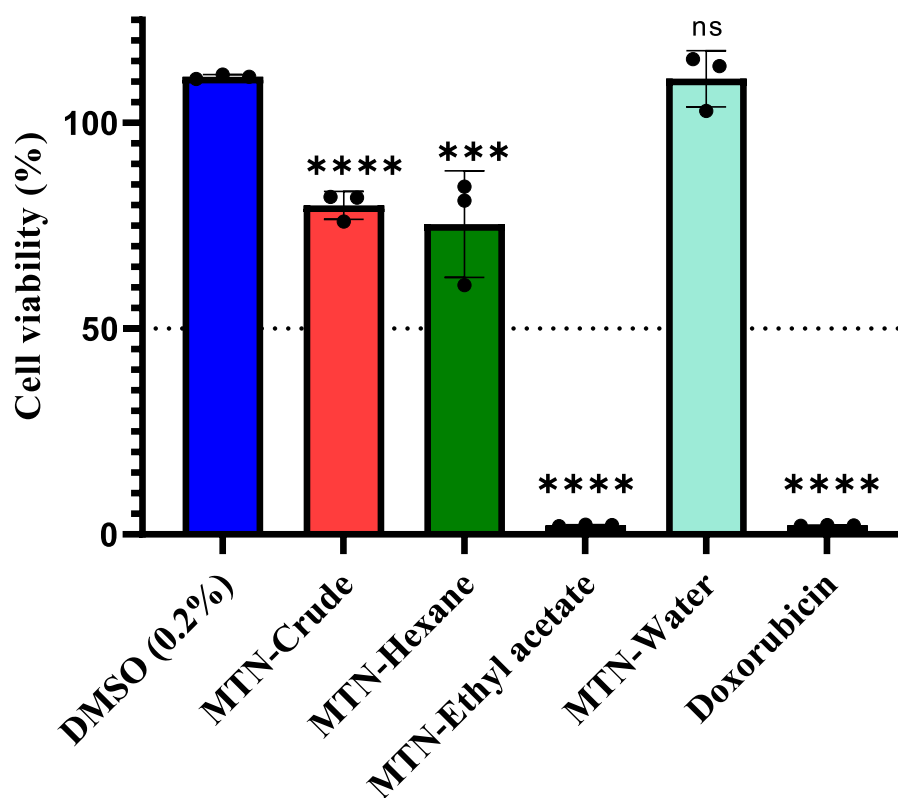
FIGURE 1
Screening of antiproliferative activity of *Launaea cornuta* extract and its fractions at a fixed concentration of 200 μg/mL on HeLa-229 cell line. Doxorubicin (200 μg/mL) was used as a positive control, and 0.2% DMSO as the negative control. All treatments were carried out in triplicate ($n = 3$). Statistical significance was calculated by nonlinear regression compared to the negative control (DMSO, 0.2%) and *, $p < 0.05$; **, $p < 0.01$, ***, $p < 0.001$ and ****, $p < 0.0001$. DMSO represents dimethyl sulfoxide; MTN represents *Launaea cornuta*.

selected as the species with a false discovery rate FDR cut-off of 0.05, and the number of pathways to be presented was set as 20. The cervical cancer (CC), molecular functions (MF), biological process (BP) and pathway enrichment terms with a *p*-value of <0.05 were identified as significantly enriched and considered for subsequent analysis.

Molecular docking

The 3D structures of AKT1 (1H10), MDM2 (5C5A), CDK2 (4GCJ), P53 (7LIN) BCL-2 (6O0O), CASP9 (4RHW) AND P21 (5DEW) were retrieved from the Protein Data Bank (https://www.rcsb.org/). The 3D structures of the *L. cornuta* compounds and the native ligands of the targeted proteins were downloaded from PubChem (https://pubchem.ncbi.nlm.nih.gov/) and converted to the PDBQT (Protein Data Bank, Partial Charge (Q), and Atom Type (T)) format using Open Babel plug-in in the PyRx software. Ligand energy minimisation was performed using the PyRx software. The grid box for each protein was maximised to fully enclose the protein structure, and blind docking was performed using the VINA tool in the PyRx, with an exhaustiveness of 8. The compounds with the binding affinity less than −7.5 kcal/mol were selected and visualised with Discovery Studio 2021 Client. Docking

validation was conducted by redocking native ligands to the target proteins.

Relative gene expression using quantitative polymerase chain reaction (qPCR) assay

In this study, a quantitative RT-PCR assay was conducted to measure the transcript levels of AKT1, TP53, BCL-2, MDM2, CDK2, Casp9, and P21 proteins. First, total RNA was extracted from HeLa cells using the SolarBio Total RNA Extraction Kit (Beijing, China) following the manufacturer's instructions. Then, the quality of the RNA was assessed using a nanodrop spectrophotometer (Thermofisher). The RNAs (1 μg) were then converted to complementary DNA (cDNA) using the SensiFAST cDNA synthesis kit (Brisbane, Australia) following the manufacturer's protocol. Quantitative RT-qPCR was performed using the SensiFAST™ SYBER® Lo-ROX Kit (Bioline, Australia). The program for the qPCR machine (QuantStudio 5; Applied Biosynthesis) was set as follows: initial denaturation at 95°C for 2 min, 1 cycle; denaturation at 95°C for 5 s, 40 cycles; annealing at 62°C for 10 s and extension at 72°C for 20 s, 40 cycles and melt curve at 60 s, 1 cycle. GAPDH was used as the reference gene and the relative expression was calculated using the $2^{-\Delta\Delta ct}$ method (Njeru

et al., 2020). The primer sequences used in this RT-qPCR analysis are presented in Supplementary Table S1.

Statistical analysis

All data described in this study were expressed as mean ± standard deviation (M±SD). GraphPad Prism 8.4 software (San Diego, CA, USA) was used to perform all the statistical analyses. Statistical comparisons were conducted using a one-way analysis of variance (ONE-WAY ANOVA), followed by the Turkey multiple comparison test. The differences were then considered statistically significant at $p < 0.05$.

Results

Screening of Launaea cornuta extract fractions for antiproliferative activity

We performed MTT assay to evaluate the antiproliferative activity of the crude *L. cornuta* extract and its solvent fractions (hexane, ethyl acetate and water fractions) at a fixed concentration (200 μg/mL) against human cervical cancer cell lines. The ethyl acetate fraction significantly ($p < 0.0001$) exhibited a robust antiproliferative effect on the HeLa cell lines, suppressing cancer cell growth by more than 50% (Figure 1). The crude extract, hexane, had significant antiproliferative effects ($p < 0.002$ and $p < 0.0001$, respectively) but not within our set tight threshold, while water fractions had no activity ($p > 0.9$) compared to the negative control. Based on these criteria, we, therefore, selected the *L. cornuta* ethyl acetate fraction for concentration-dependent tests to obtain the minimum inhibitory concentration (IC_{50}).

Dose-dependent cytotoxicity

A dose-dependent cytotoxicity test was performed to determine the concentration of the *L. cornuta* ethyl acetate fraction that selectively inhibited the growth of Hela cells by determining both IC_{50} and CC_{50}) (Figures 2, 3). HeLa cells and Vero cells were treated with ethyl acetate fraction of *L cornuta* at concentrations ranging from 1–64 μg/mL (HeLa cells) and 4–256 μg/mL (Vero cells). After 48 h, *L. cornuta* ethyl acetate IC_{50} and CC_{50} for HeLa and Vero cells were determined as 20.56 ± 2 μg/mL and 48.83 ± 23 μg/mL, respectively. Doxorubicin exhibited an IC_{50} of 2.09 ± 1.35 μg/mL on Hela cells and a CC_{50} of 3.44 ± 1.00 μg/mL on Vero cells, respectively (Table 1). The dose-dependent test results for positive control (doxorubicin) are presented in the Supplementary Figure S1.

Selectivity index (SI) was calculated to assess the selective toxicity of *L. cornuta* ethyl acetate fraction toward cervical cancer cells compared to normal cells. The resulting SI value for the HeLa cell was 2.37 and 1.64 for *L. cornuta* ethyl acetate fraction and doxorubicin, respectively (Table 1; Figure 4), demonstrating high selectivity of *L. cornuta* ethyl acetate fraction to cancer cells.
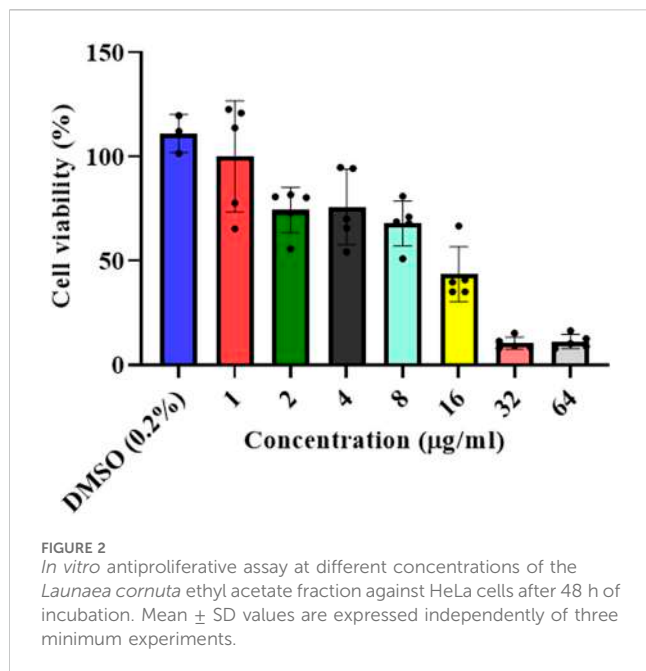
Morphological study

We confirmed the effect of *L. cornuta* ethyl acetate fraction on the morphology of HeLa cells for 48 h under a digital microscope. HeLa cells exposed to varying concentrations of *L. cornuta* ethyl acetate fraction exhibited atypical morphology with cellular shrinkage, sphere-shaped and surface detachment, indicating that the extract fraction had cytotoxic effects (Figure 5) as compared to the negative control. Notably, the effects of the extract fraction was dose-dependent.

Effect of Launaea cornuta ethyl acetate on cell migration

A wound-healing assay was conducted to investigate the effect of *L. cornuta* ethyl acetate fraction on cancer cell migration. The results indicated a decrease in wound size in the control cells (DMSO, 0.2%), which eventually closed after 48 h compared with treated HeLa cells. In contrast, the HeLa cells treated with *L. cornuta* ethyl acetate fraction at IC_{50} of 20.56 μg/mL inhibited wound closure. The results indicated that *L. cornuta* ethyl acetate significantly ($p < 0.0001$) inhibited cell migration compared to the negative control after 24 and 48 h. However, there were no significant differences between *L. cornuta* ethyl acetate and the positive control at 24 and 48 h ($p > 0.6$ and $p > 0.9$, respectively). The substantial decrease in migration and minimum closure in wound size was attributed to the increased cell mortality and/or inhibition of cell migration mediated by the extract fraction (Figure 6A). The percentage of wound closure for *L. cornuta* ethyl acetate fraction (20.56 μg/mL) was 35.9% and 41.9% for 24 and 48 h (Figure 6B).

Preliminary screening and gas chromatography-mass spectrometry (GC-MS) analysis of phytochemicals in L. cornuta ethyl acetate

Having demonstrated selective antiproliferative activity of *L. cornuta* ethyl acetate, we next then identified the phytochemicals that could be attributed to the established antiproliferative activity of the extract fraction. The qualitative phytochemical screening showed broad groups of phytochemicals as follows: glycosides, phenols, saponins, terpenoids, quinones, and tannins (Supplementary Table S2). GC-MS analysis was performed to reveal the semi-quantitative presence of phytochemical profiles. A total of 13 compounds were identified in *L. cornuta* ethyl acetate fraction through GC-MS analysis (Table 2), and the chromatogram showing the 13 peaks is presented in the Supplementary Figure S2. The compounds identified included (9Z,12Z) -octadeca-9,12-dienoyl chloride (57.26%), 2-Octylcyclopropene-1-heptanol (14.48%), Tricyclo [20.8.0.0 (7,16)] triacontane, 1 (22) 7, 7 (16) -diepoxy, Tricyclo [20.8.0.0 (7,16)] triacontane, 1 (22) 7, (16)-diepoxy (7.39%), ethyl (9Z,12Z,15Z)-octadeca-9,12,15-trienoate (4.28%), Cycloprop [e]indene-1a,2(1H)-dimethanol, 3a,4,5,6,6a,6b-hexahydro-5,5,6b-trimethyl-, (1a.alpha,3a.beta,6a.beta,6b.alpha) (2.94%), 6-Hydroxy-4,4,7a-trimethyl-5,6,7,7a-tetrahydrobenzofuran-2(4H)-one (2.73%) and 2-Linoleoylglycerol (2.28%). A previous study

FIGURE 2
In vitro antiproliferative assay at different concentrations of the *Launaea cornuta* ethyl acetate fraction against HeLa cells after 48 h of incubation. Mean ± SD values are expressed independently of three minimum experiments.

reported that 6-Hydroxy-4,4,7a-trimethyl-5,6,7,7a-tetrahydrobenzofuran-2(4H)-one exhibited anti-inflammatory effect against lipopolysaccharide (LPS)-induced raw macrophage (Jayawardena et al., 2019), Glycerol 1,2-dipalmitate possess ant-fungal activity (Sanni and Omotoyinbo, 2016). Ethyl (9Z,12Z,15Z)-octadeca-9,12,15-trienoate exhibited anticancer activity against oral epidermoid carcinoma,

breast, colon, and lung cancer (Huang et al., 2022), Stigmast-5-ene, 3beta-methoxy- induced a reduction of cell viability by apoptotic cell death through cell cycle arrest at the sub-G1 stage (Alvarez-sala et al., 2019; Jaiganesh et al.) and tremulone exhibited anticancer activity against cervical, colorectal and breast cancers (Lu et al., 2012; Suliman and El-hddad, 2023). However, most of the compounds identified in this study have not been reported to have biological activity, therefore, further investigation is necessary to evaluate the potential biological activity of each compound. The 2D structures of these compounds are shown in Figure 7.

In-silico results

Screening for drug-like compounds in *Launaea cornuta* ethyl acetate fraction

The chemical compounds of *L. cornuta* ethyl acetate fraction obtained from GC-MS analysis were used in the *in silico* studies. Thirteen compounds were subjected to screening, and their putative pharmacokinetics and physicochemical properties (absorption, distribution, metabolism, excretion and toxicity) were determined using SwissADME and pkCSM databases. Only 6 met the Lipinski's rule of 5 (RO5) of MW; <500 g/mol, Log P; <5, HBA<10, HBD<5, and RB < 10. In addition to Lipinski's rules, the compounds were also predicted to be water-soluble and did not interfere with the blood-brain barrier and nervous system. Furthermore, the ADMET profile suggest that the 6 compounds do not interfere with metabolism, thus minimising the risk of drug-drug interactions
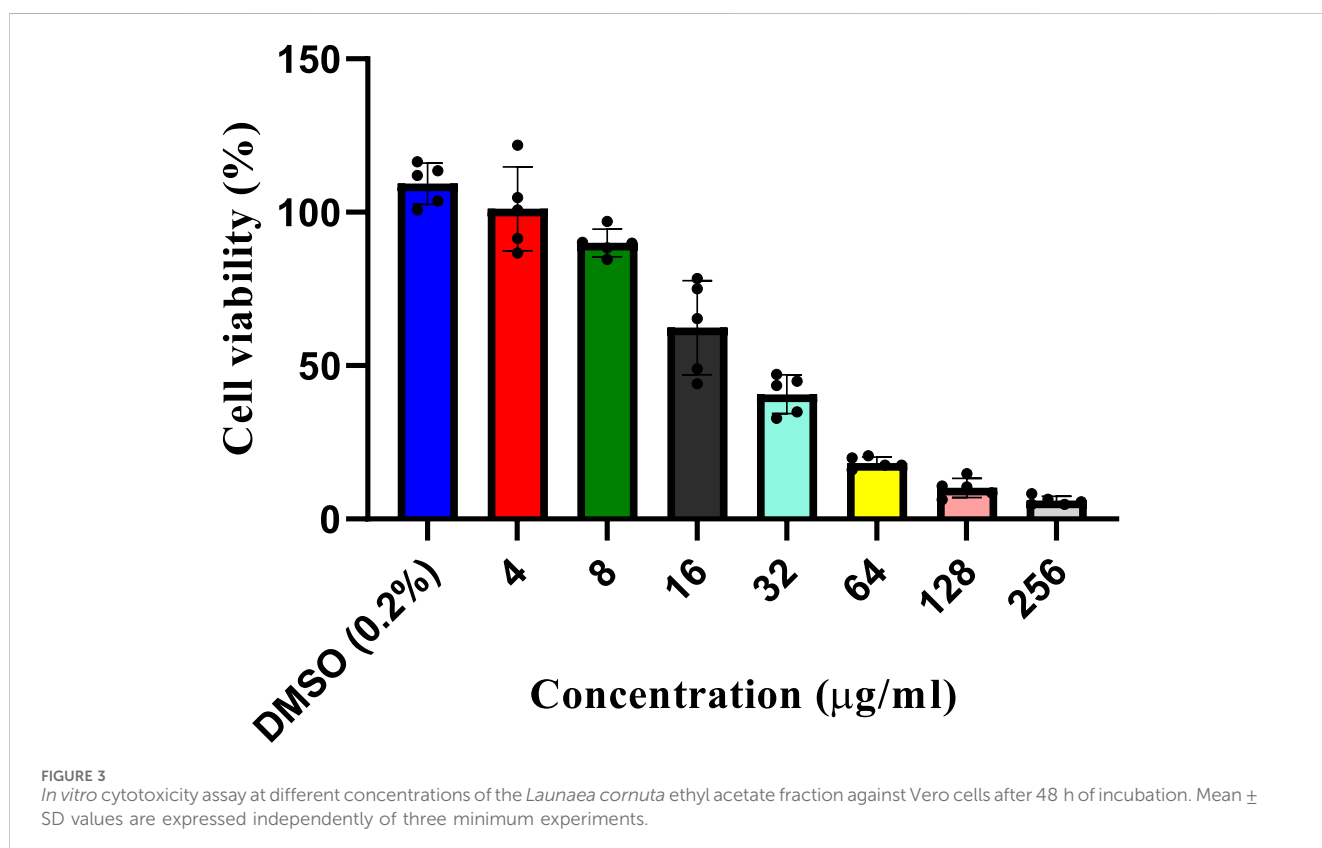

FIGURE 3
In vitro cytotoxicity assay at different concentrations of the *Launaea cornuta* ethyl acetate fraction against Vero cells after 48 h of incubation. Mean ± SD values are expressed independently of three minimum experiments.

TABLE 1 Selectivity Index (SI) of *Launaea cornuta* ethyl acetate fraction and doxorubicin.

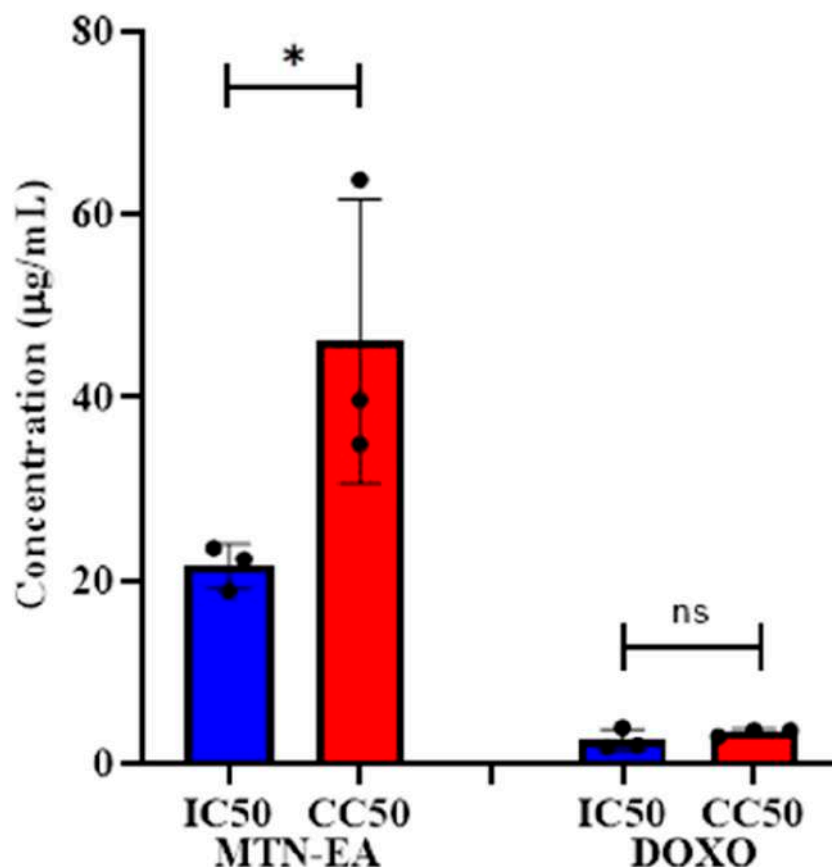| Extract	IC$_{50}$ (µg/mL)	CC$_{50}$ (µg/mL)	SI
L. cornuta ethyl acetate fraction	20.56 ± 2.83	48.83 ± 23.02	2.36
Doxorubicin	2.09 ± 1.35	3.44 ± 1.00	1.64

FIGURE 4
Half-maximal concentration and half-maximal cytotoxic concentration of *Launaea cornuta* ethyl acetate and doxorubicin on HeLa and Vero cells after 48 h of incubation. There is a significant difference between IC$_{50}$ and CC$_{50}$ values ($p < 0.01$). Mean ± SD values are expressed independently of three minimum experiments.

(Table 3, Supplementary Table S3). Oral bioavailability was evaluated for the six (6) compounds using a bioavailability radar (Ahmed Khan et al., 2023) (Figure 8). The bioavailability radars were based on six ideally adapted physicochemical properties for oral bioavailability, namely, lipophilicity, polarity, size, solubility, saturation, and flexibility. The thresholds were as follows: lipophilicity (LIPO): 0.7 < XLOGP3 < +5, SIZE: 150 < MV < 500 g/mol, flexibility (FLEX): 0 < Number of rotatable bonds <9, saturation (INSATU): 0.25 < Fraction Csp3 < 1, insolubility (INSOLU): 6 < LOG S < 0, and polarity (POLAR): 20 Å2 < TPSA < 130 Å2. All candidate molecules exhibited oral bioavailability because they were within the pink zone of bioavailability radars. The pink-coloured area presents the fit physicochemical space for oral bioavailability. The graph for each molecule must be adjusted to suit drug-like properties. The prediction of ADMET pharmacokinetic properties demonstrated

that all six compounds exhibited good absorption properties as their human intestinal absorptions (HIAs) exceeded 90%. The inhibitory effect on cytochromes indicated that most of them did not affect cytochromes except M5, M7, M11 and M12, which inhibited 3A4, whereas M7, M11, and M12 inhibited 1A2 (Table 3). The ADMES toxicity confirmed that the six drug candidates were not toxic inhibitors. M5, M8, and M11 were predicated to be sensitive to the skin but had no hepatotoxic effect except M13.

Prediction of targets for *Launaea cornuta* ethyl acetate compounds and cervical cancer

The putative targets of the six (6) compounds of *L. cornuta* ethyl acetate fraction were predicted and retrieved from three databases:
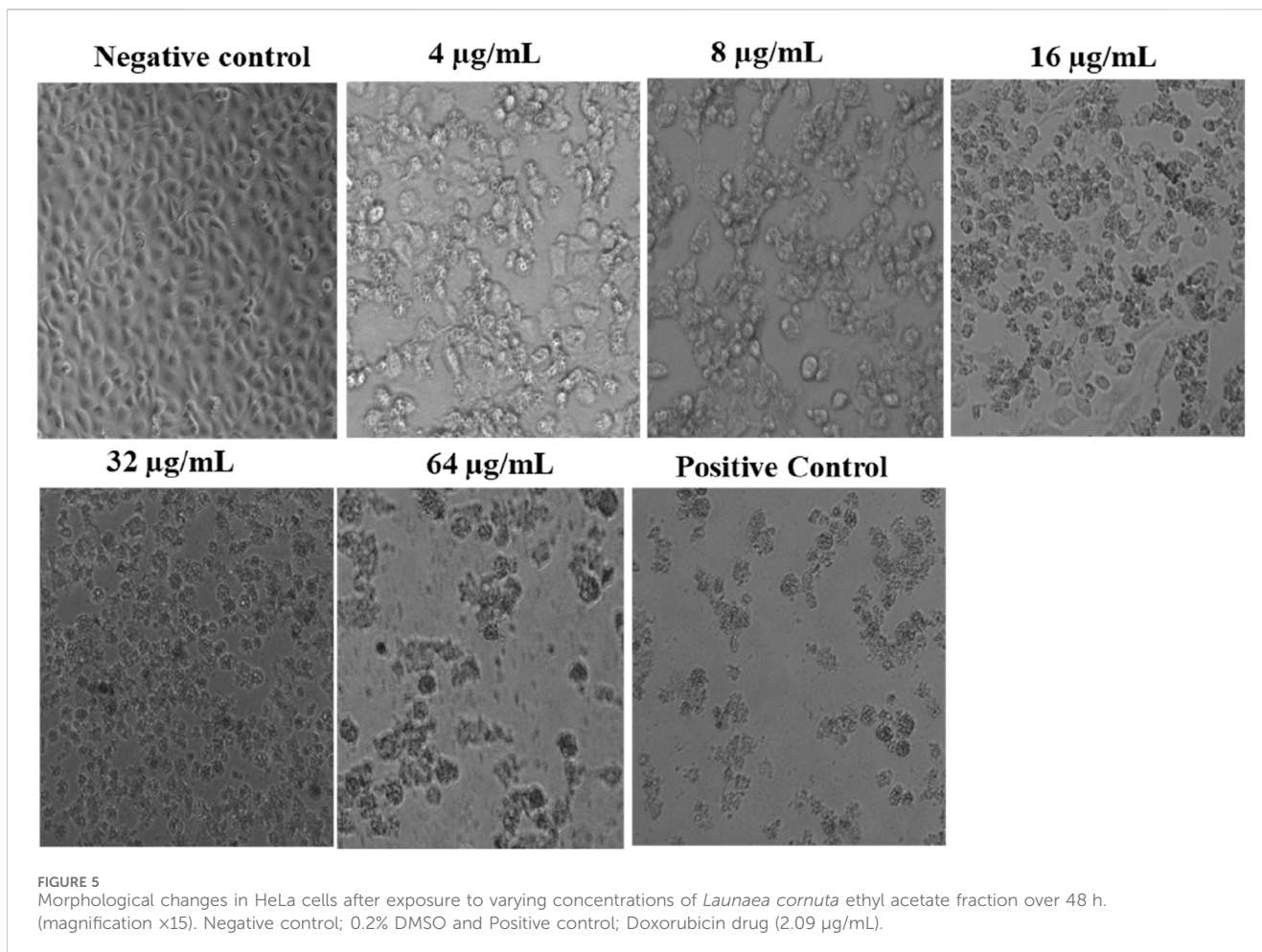
FIGURE 5
Morphological changes in HeLa cells after exposure to varying concentrations of *Launaea cornuta* ethyl acetate fraction over 48 h. (magnification ×15). Negative control; 0.2% DMSO and Positive control; Doxorubicin drug (2.09 μg/mL).

SWISS TargetPrediction (STP) with 612 targets, BindingDB (BDB) with 59 targets, and the Similarity Ensemble Approach (SEA) with 503 targets. The targets obtained were merged to obtain 581 unique potential targets. We also predicted human cervical cancer-related genes from 4 databases: GeneCards with 714 targets, DisGeNET with 1817 targets, Pharos with 174 targets, and OMIM with 50 targets to obtain 2253 unique targets. A Venn diagram was generated to show the intersected targets between *L. cornuta* ethyl acetate fraction and cervical cancer as hub genes for subsequent analyses (Figure 9A).

Construction of protein-protein interaction (PPI) network for the compound-disease targets

The intersected targets obtained using the Venn tool were imported into the STRING database. Cytoscape 3.10 software was used to construct a PPI network, as shown in Figure 9B. The top 30 key hub targets were selected according to their degree and score ranking using the Cytohubba plugin: the greater the degree value, the larger the node (Supplementary Table S4). The PPI exhibited 124 nodes and 1,457 edges. The average node degree and Local Clustering Coefficient were 23.5 and 0.61, respectively. The expected number of edges was 720. The PPI enrichment p-value

was <1.0e-16, implying there were more interactions of the proteins than expected. This could also indicate that proteins are biologically linked as cluster proteins. The top 30 hub genes are shown in Figure 10. Among the top 30 targets, AKT1, MDM2, and CDK2 were selected as therapeutic targets in cervical cancer due to their established roles in the regulation of apoptosis and BCL2, Caspase9, TP53 and P21 due to their established role in the regulation and progression of the cell cycle and apoptosis (Rashmi et al., 2014; Li et al., 2023; Tatekawa et al., 2024).

Gene ontology enrichment analysis

GO and KEGG enrichment analyses were conducted for the 124 intersection targets using ShinyGO 0.77 server (restricted species: *H. sapiens*; $p < 0.05$), and a total of 1415 GO enrichment terms were retrieved. The GO terms were classified into three categories with 1,234 terms in the biological processes (BP) category, 88 in the cellular (CC) category and 93 in the molecular functions (MF) category. The top 20 significant GO terms for each GO category were selected (Figure 11). The top enriched biological processes mainly included MAP Kinase cascade, regulation of programmed cell death and apoptotic processes, response to both organic cyclic compounds and hormones, cellular response to oxygen-containing
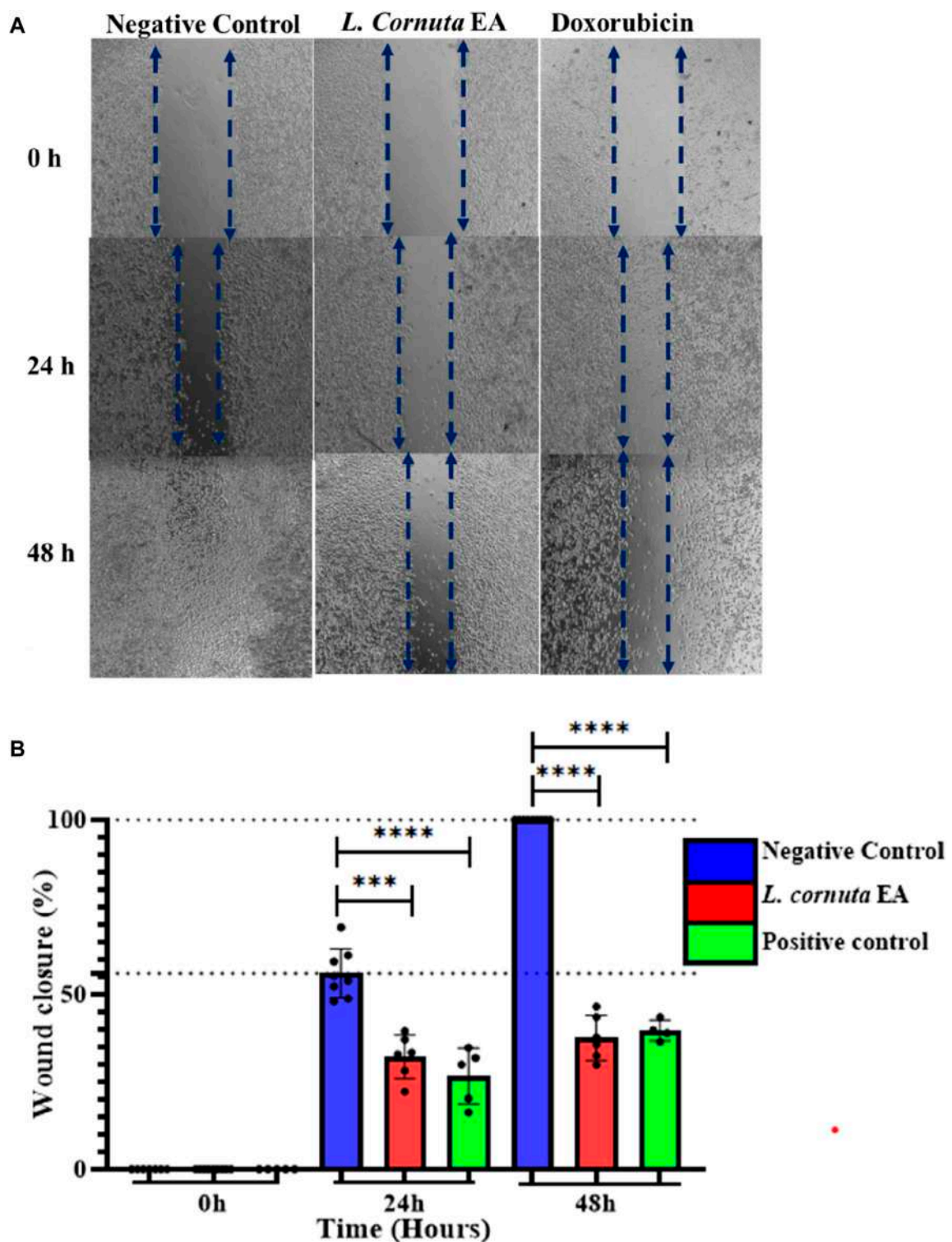
FIGURE 6
Launaea cornuta ethyl acetate inhibited HeLa cells migration ability after treatment at a concentration of 20.56 μg/mL (IC$_{50}$). Images were obtained at time points of 0, 24, and 48 h were taken to capture images. **(A)** photomicrographs show the anti-migration effects of *Launaea cornuta* ethyl acetate fraction on HeLa cells as compared with negative control. **(B)** Percentage of wound healing area. Each bar graph shows the wound closure (%) of HeLa cells. Wound areas were measured at each time point and expressed as a percentage of reduction area in comparison with 0 h of incubation. The percentages of wound closure were statistically compared to the negative control. Each bar represents mean $\pm$ SD of at least three independent experiments performed in triplicate. ***, $p < 0.001$ and ****, $p < 0.0001$.

TABLE 2 The phytochemical profile of the *Launaea cornuta* ethyl acetate fraction detected by the GC-MS technique.

Peak no.	RT (minute)	Compound	MF	MW (g/ mol)	Relative abundance (%)	Type of compound
1	16.476	6-Hydroxy-4,4,7a-trimethyl-5,6,7,7a-tetrahydrobenzofuran-2(4H)-one	$C_{11}H_{16}O_3$	196.2	2.73	Benzenoids
2	21.249	Glycerol 1,2-dipalmitate	$C_{35}H_{68}O_5$	568.9	1.57	Fatty acid methyl esters
3	21.955	Cycloprop [e]indene-1a,2(1H)-dimethanol, 3a,4,5,6,6a,6b-hexahydro-5,5,6b-trimethyl-, (1a.alpha.,3a.beta.,6a.beta.,6b.alpha.)-(−)-	$C_{15}H_{24}O_2$	236.4	2.94	Terpenoids
4	22.006	3-Heptafluorobutyriloxy-3,5,10-pregnatrien-20-one	$C_{25}H_{27}F_7O_3$	505.8	1.21	Aliphatic compound
5	22.361	2-Linoleoylglycerol	$C_{21}H_{38}O_4$	354.5	2.28	Glycerolipids
6	22.791	2-Octylcyclopropene-1-heptanol	$C_{18}H_{34}O$	266.5	14.48	Fatty alcohols
7	23.798	Tremulone	$C_{29}H_{46}O$	410.7	1.26	Terpenoids
8	24.799	Spiro [2.6]non-4-ene, 4-ethyl-8-methylene-5-trimethylsilyl	$C_{15}H_{26}Si$	234.5	1.98	Alkenes
9	26.127	Cyclohexyldichlorophosphine	$C_6H_{11}Cl_2P$	185.0	0.96	Fatty acids
10	26.127	(9Z,12Z)-octadeca-9,12-dienoyl chloride	$C_{18}H_{31}ClO$	298.9	57.26	Fatty acids
11	27.018	Ethyl (9Z,12Z,15Z)-octadeca-9,12,15-trienoate	$C_{20}H_{34}O_2$	306.5	4.28	Fatty acids
12	29.624	Stigmasteryl methyl ether	$C_{30}H_{52}O$	428.7	1.67	Phytosterols
13	31.846	Tricyclo [20.8.0.0 (7,16)]triacontane, 1(22),7(16)-diepoxy	$C_{30}H_{52}O_2$	444.7	7.39	Fatty acids

Key: RT, retention time (minute); MF, molecular formula; MW, molecular weight (g/mol).

compounds, and positive regulation of cell population proliferation. The most enriched cellular compounds terms included phosphatidylinositol 3-kinase complexes I and IA, endosome, receptor complexes, transferase complex, and membrane raft, and the significantly enriched molecular function terms mainly associated with the core targets included nuclear receptors, ligand-activated transcription factors, transmembrane receptor protein tyrosine kinase, and protein tyrosine kinase activities.
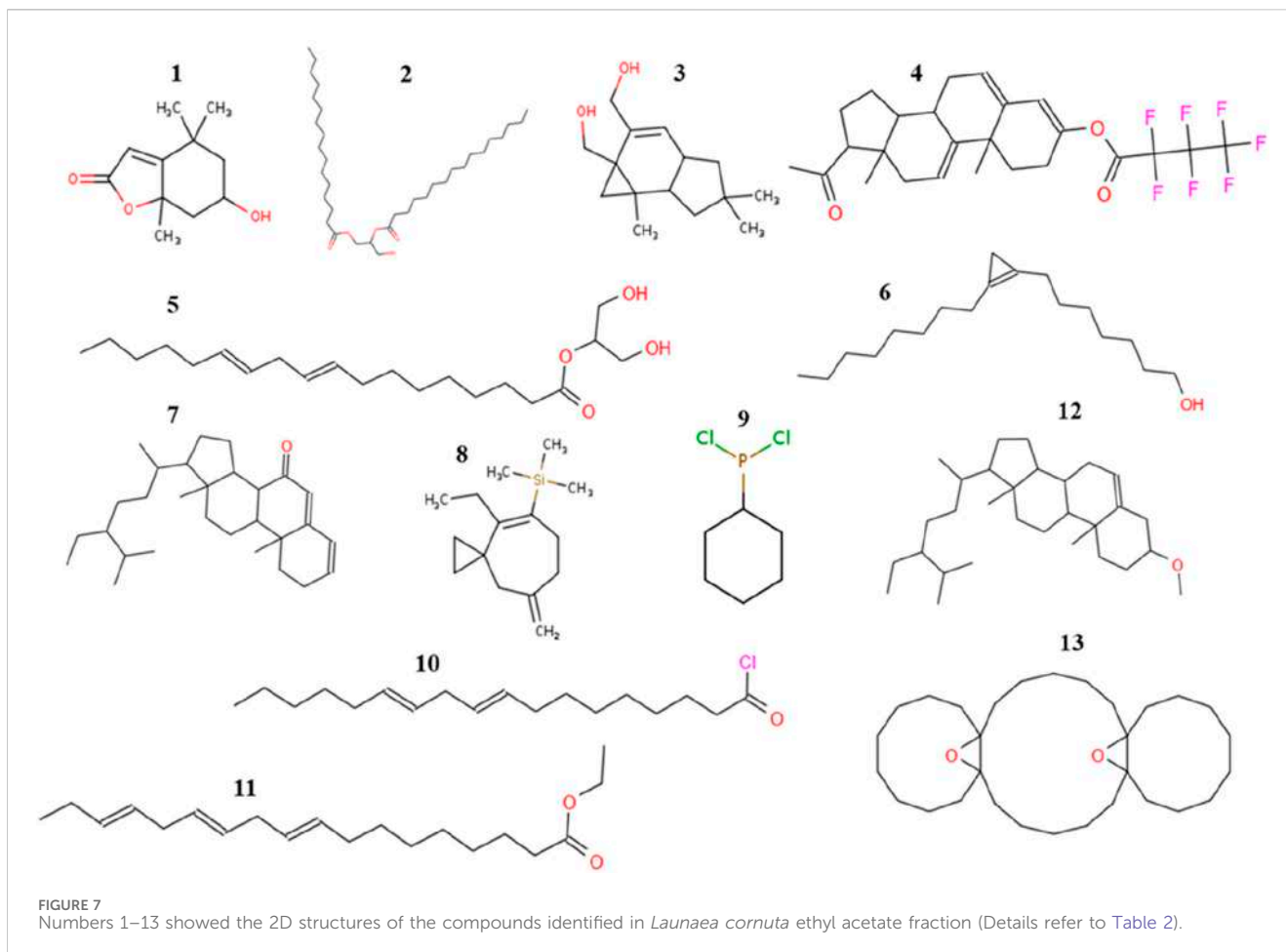
Kyoto encyclopaedia of genes and genomes pathway enrichment analysis

KEGG pathway analysis was performed to explore the pathways associated with the anticervical cancer effect of the *L. cornuta* ethyl acetate-related target genes. The results showed that 124 target genes were associated with enriched in 123 significantly enriched pathways ($p > 0.05$). This implies that the anticervical cancer mechanism of *L. cornuta* ethyl acetate involves multiple targets, genes, and pathways. The top 20 KEGG signalling pathways with lower *p*-values were selected as the significant pathways (Figure 12; Supplementary Table S5). The top enriched cancer-associated pathways included central carbon metabolism in cancer, Ras signalling pathway, FoxO signalling pathway and PI3K-Akt signalling pathway. The PI3K-AKT signalling pathway with a lower *p*-value was predicted to be highly associated with cervical cancer and was selected for

subsequent analysis. The KEGG pathway mapped to link molecular interaction, reactions, and relation network associated with top enriched pathway are presented in Figure 13. The proposed pathway model-based on the selected targets is presented in Figure 14.

Molecular docking results

Molecular docking was performed to stimulate the possibility of binding and interactions between *L. cornuta* ethyl acetate fraction compounds and the core targets in cervical cancer using PyRx software. Six (6) compounds of *L. cornuta* ethyl acetate fraction were docked against 7 target proteins (Supplementary Table S6). We selected 3 target proteins (AKT1, CDK2, and MDM2 from the top core hub genes and 4 target proteins (BCL2, TP53, P21, and Casp9) due to their established roles in regulating cell cycle and apoptosis (Xing et al., 2015; Yuan et al., 2018; Ghosh et al., 2020; Luo et al., 2023). Two ligands, stigmasteryl methyl ether (M12) and tremulone (M7), that exhibited binding affinity less than −7.0 kcal/mol with zero (0) root mean standard deviation (RMSD), were selected, analysed and presented in Supplementary Table S7 and Supplementary Figure S3. Molecular docking results indicated that stigmasteryl methyl ether and tremulone ligands exhibited good binding affinity with the selected target proteins (CDK2-M12 with −12.6 kcal/mol, MDM2-M12 with −9.1 kcal/mol, BCL2-M12 with −10.3 kcal/mol, Casp9-M7 with −9.9 kcal/mol, P21-M7 with −8 kcal/mol, TP53-M7 with −7 kcal/mol and AKT-

FIGURE 7
Numbers 1–13 showed the 2D structures of the compounds identified in *Launaea cornuta* ethyl acetate fraction (Details refer to Table 2).

M12 with −9.5 kcal/mol respectively). Their interactions were mainly through several hydrogen and hydrophobic bonds (Figures 15 and 16).
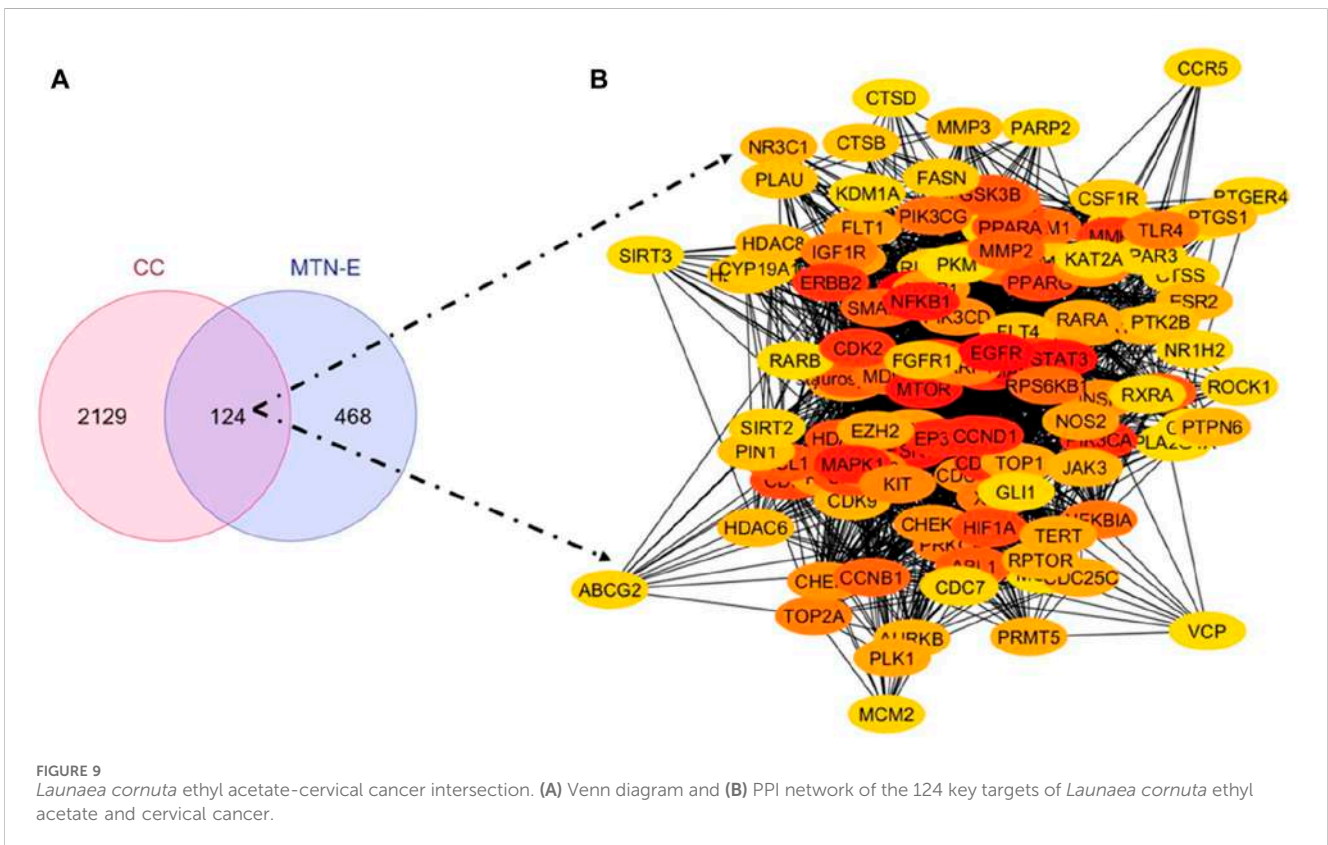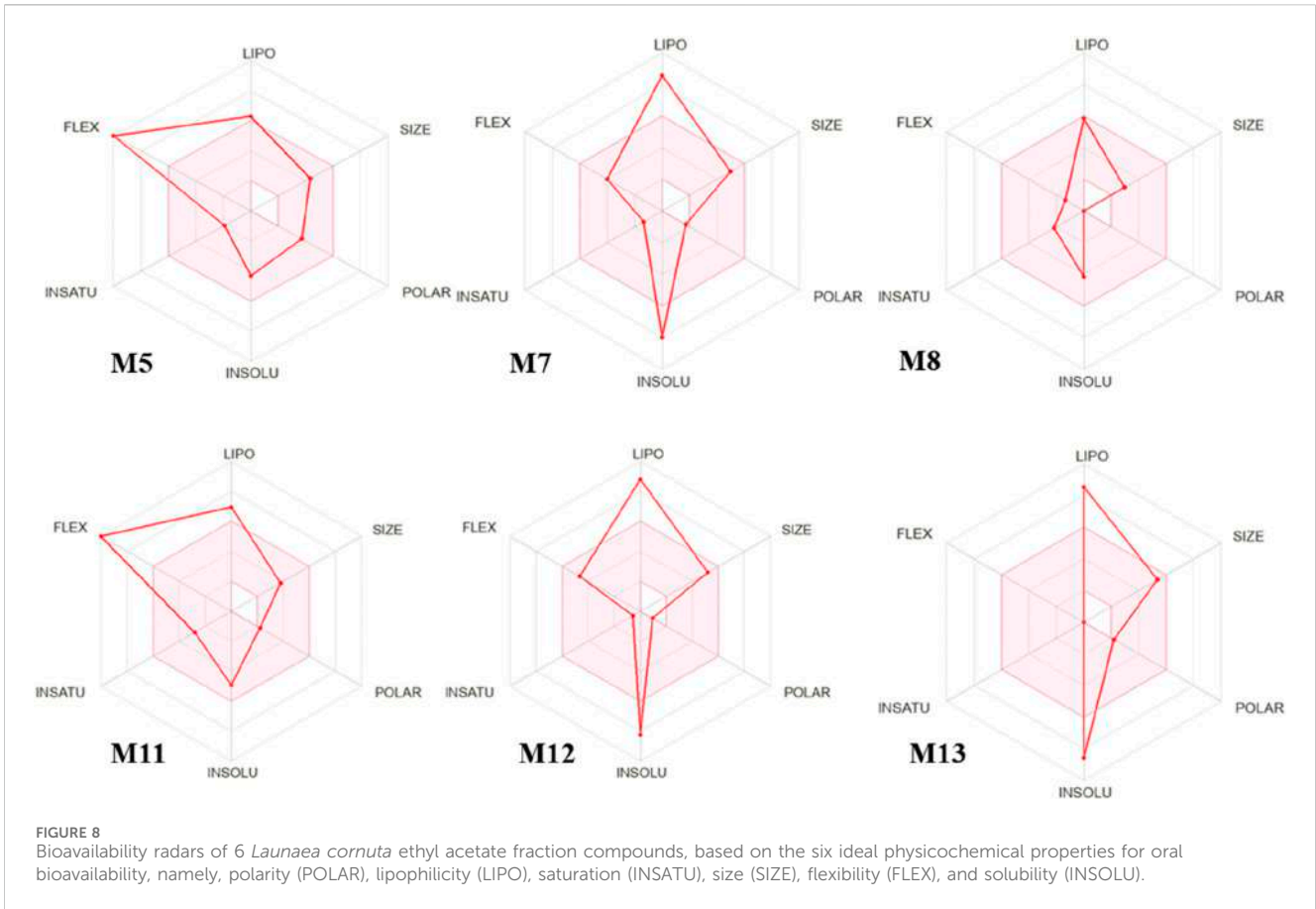
The redocked results for the native ligands with their target proteins are presented in Supplementary Figure S4 and Supplementary Table S8. M12 bonds to AKT1 protein through one hydrogen interaction with residue Glu40A and two hydrophobic interactions with residues His13A and Trp11A. Meanwhile, the native ligand NL7 interacted with AKT1 protein (−5.2 kcal/mol) through several hydrogen bonds with residues Lys20A, Arg15A, and Glu17A and hydrophobic interactions with residues Glu85A, Glu17A, Lys20A and Arg15A. The interaction between M12 and MDM2 protein occurred through hydrophobic bonds only with interacting residues of Val109A, Tyr104A, and Arg105A, whereas the native ligand NL2 bind to MDM2 (−7.3 kcal/ mol) through one hydrogen bond with residues Hu8201A and hydrophobic interactions with residues Hu8201A and Lys51A. M12 bind to CDK2 protein through one hydrogen interaction with residue Leu55A and hydrophobic interactions with residues Thr15A, Ala151A, Leu148A, Phe152A, and Ile35A. CDK2 interacted with its co-recrystallised ligand NL1 (−9.3 kcal/ mol) through a number of hydrogen interactions with residues Thr14A, Gln131A, Glu12A, Asp145A, Asp127A, Phe146A, Lys33A and Leu148A as well as several hydrophobic interactions with residues Ala151A, Ile35A, Lys33A, Leu148A, Tyr15A,

Asp127A and Asp145A respectively. BCL2 protein interacted with M12 through several hydrophobic interactions with residues Trp135C, Phe89C and Ala90C, while the native ligand NL3 binds to BCL2 (−8.1 kcal/mol) through two hydrogen bonds with residues Arg142A and His143A and hydrophobic bonds through residues Arg86A, Ala90A, Phe89A and Glu138A. The interaction between M7 and Casp9 occurred through residue Arg44C to form a hydrogen bond and residue Ile43 to form a hydrophobic bond. Conversely, the native ligand NL4 interacted with Casp9 protein (−9.3 kcal/mol) through several hydrogen bonds with residues Arg44C, Arg52C, Asn45C, Glu46C, Ser48E, and Pro47A only. M7 bind to TP53 protein through two hydrogen bonds with residues Tys134 and Tys135 and through residue Lys134 to form a hydrophobic interaction. The co-recrystallised ligand NL6 (−8 kcal/mol) interacted through residues Lys129A and Gly132A to form hydrogen bonds and through residues Met117A, Phe102A, Phe133A and Tyr123A to form hydrophobic bonds and lastly, the interaction between P21 and M7 occurred through residues Lys308A, Leu311A, A:59N601 forming hydrophobic bonds only whereas the native ligand NL5 (−8.5 kcal/mol) had interaction through residues Gly409A, Glu423A and Asp393A to form two hydrogen bonds and hydrophobic bonds with residues Leu311A, Phe410A and Ile312A. These results showed that CDK2-M12, BCL2-M12, Casp9-M7 and P21-M7 complexes shared the same active site residues implicated in the binding of the native ligand for

TABLE 3 Prediction of ADMET *in silico* pharmacokinetic properties of *Launaea cornuta* ethyl acetate compounds.

Compounds number	Absorption	Distribution		Metabolism							Excretion	Toxicity		
	Intestinal absorption (human)			Substrate	Inhibitor						Total excretion			
		Permeability		Cytochromes										
		BBB	CNS	2D6	3A4	1A2	2C19	2C9	2D6	3A4		Ames toxicity	Hepatotoxicity	Skin irritation
	Numeric (% absorbed)	Numeric (log BB)	Numeric (log PS)	Categorical (yes/No)							Numeric (log mL/minute/kg)	Categorical (yes/No)		
M1	95.697	−0.198	−3.36	No	No	No	No	No	No	No	1.038	No	No	Yes
M2	85.807	−0.943	−3.114	No	Yes	No	No	No	No	No	2.171	No	No	No
M3	92.7	0.091	−2.37	No	No	No	No	No	No	No	−0.007	No	No	No
M4	91.346	0.185	−3.244	No	Yes	No	No	No	No	No	−0.103	No	No	No
M5*	90.602	−0.294	−3.227	No	Yes	No	No	No	No	No	2.165	No	No	Yes
M6	90.308	0.837	−1.802	No	Yes	No	No	No	No	No	1.715	No	No	Yes
M7*	97.921	0.827	−1.589	No	Yes	Yes	No	No	No	No	0.571	No	No	No
M8*	93.522	0.763	−2.141	No	No	No	No	No	No	No	1.11	No	No	Yes
M9	90.275	0.684	−1.794	No	No	No	Yes	No	No	No	0.418	No	No	No
M10	91.195	0.81	−1.394	No	Yes	No	No	No	No	No	0.237	No	No	No
M11*	92.747	0.766	−1.509	No	Yes	Yes	No	No	No	No	2.134	No	No	Yes
M12*	96.946	0.903	−4.387	No	Yes	Yes	No	No	No	No	0.663	No	No	No
M13*	91.183	1.466	−3.114	No	Yes	No	No	No	No	No	0.909	No	Yes	No

Key: BBB, Brain-blood barrier; CNS, central nervous system; ADMET, absorption, distribution, metabolism, excretion, and toxicity; * Drug-like compounds (DL).
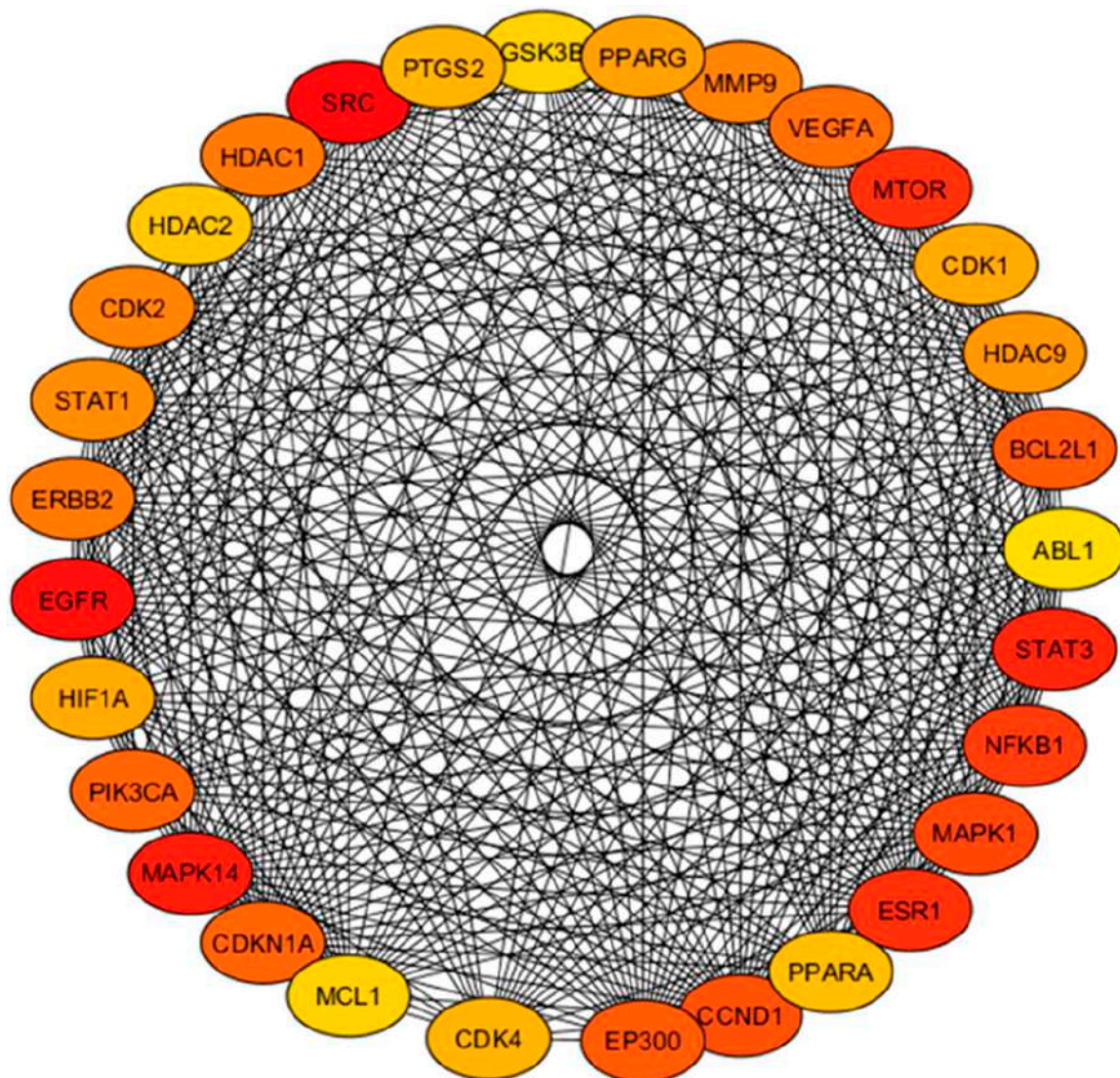
FIGURE 8
Bioavailability radars of 6 *Launaea cornuta* ethyl acetate fraction compounds, based on the six ideal physicochemical properties for oral bioavailability, namely, polarity (POLAR), lipophilicity (LIPO), saturation (INSATU), size (SIZE), flexibility (FLEX), and solubility (INSOLU).

FIGURE 9
Launaea cornuta ethyl acetate-cervical cancer intersection. **(A)** Venn diagram and **(B)** PPI network of the 124 key targets of *Launaea cornuta* ethyl acetate and cervical cancer.

FIGURE 10
PPI network for the top hub targets. The top 30 targets selected from *Launaea cornuta* ethyl acetate-cervical cancer targets. The intensity of the colour represents the significance ($p < 0.05$) of the targets, with darker red indicating a higher degree.

each protein, whereas ATK1-M12, MDM2-M12 and TP53-M7 complexes did not share any active site residues implicated in the binding of native ligands.

The effect of *L. cornuta* ethyl acetate fraction on mRNA expression levels of selected target genes in HeLa cells

Real-time PCR analysis was performed to validate the putative molecular targets of *L. cornuta* ethyl acetate fraction associated with the cervical cancer cells, as depicted by the network analysis results. We evaluated the gene expression levels of ATK1, BCL2, CDK2, MDM2, P21, TP53, and Casp9 in HeLa cells treated with *L. cornuta* ethyl acetate fraction and untreated HeLa cells. AKT1, CDK2 and MDM2 were among the top hub genes. We further selected BCL2, P21, TP53 and Casp9 genes due to their established

role in apoptosis and cell cycle. The quantification cycle, also known as the threshold cycle (Ct), was determined, and relative gene expression levels of the target genes were normalized to GAPDH (Figure 17). There was significant upregulation of Casp9 ($p < 0.0001$) and P21 ($p < 0.5$) expression levels in HeLa cells treated with *L. cornuta* ethyl acetate fraction compared to the negative control (NC). There was a significant downregulation of BCL-2 ($p < 0.01$), MDM2 ($p < 0.0001$), and CDK2 ($p < 0.01$) expression levels in the *L. cornuta*-treated cervical cancer cells compared to the NC. The gene expression level of TP53 was upregulated, although the difference was not significant ($p > 0.0591$) in treated HeLa cells compared to the NC. Meanwhile, there was no significant expression level of AKT1 ($p > 0.1452$) in the *L. cornuta*-treated cervical cancer cells compared to the NC. The RT-qPCR results suggest the fact that *L. cornuta* ethyl acetate fraction interferes with cervical cancer cell proliferation by inducing cell cycle arrest and apoptosis.
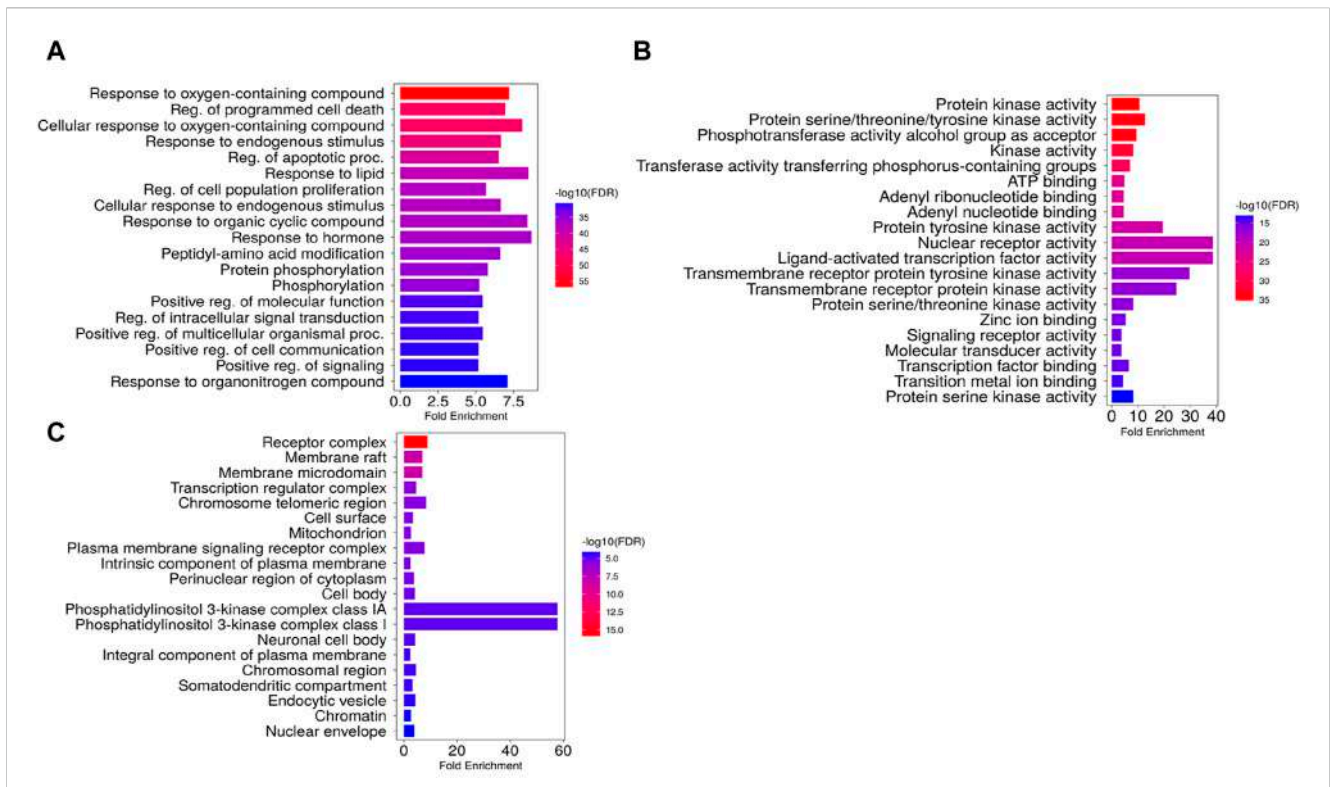
FIGURE 11
Gene Ontology enrichment terms associated with *Launaea cornuta* ethyl acetate compounds. **(A)** biological process terms, **(B)** molecular function terms, and **(C)** cellular component terms. The bar represents the GO terms on the vertical axis. The LogP values are shown on the horizontal axis. The enrichment colour scale defines the FDR, with red colour indicating a high FDR value and a significant association.
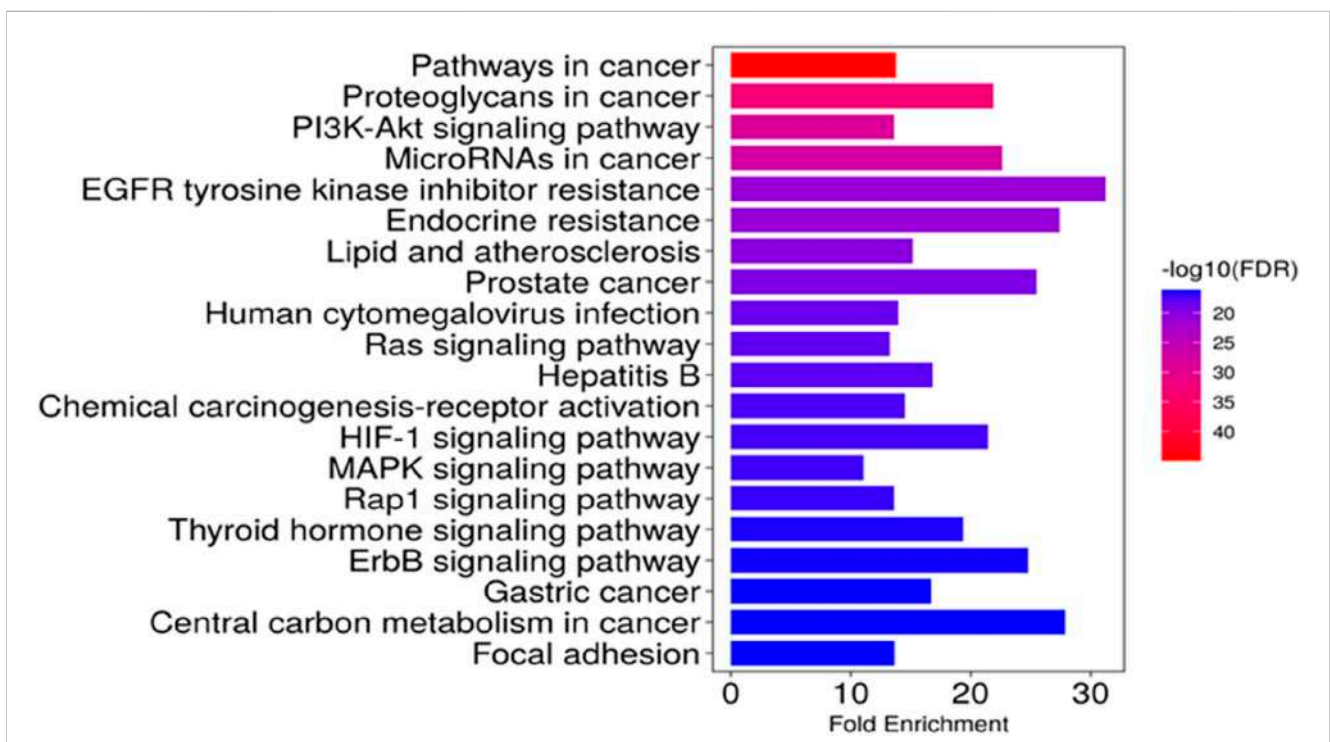

FIGURE 12
Kyoto Encyclopedia of Gene and Genomes (KEGG) pathway enrichment analysis. A) the enriched pathway associated with *Launaea cornuta* ethyl acetate targets. The bar represents the KEGG terms on the vertical axis. The LogP values are shown on the horizontal axis. The enrichment colour scale defines the FDR, with red colour indicating a high FDR value and a significant association.

FIGURE 13
Enriched KEGG pathways associated with cervical cancer-related targets of *Launaea cornuta* ethyl acetate.
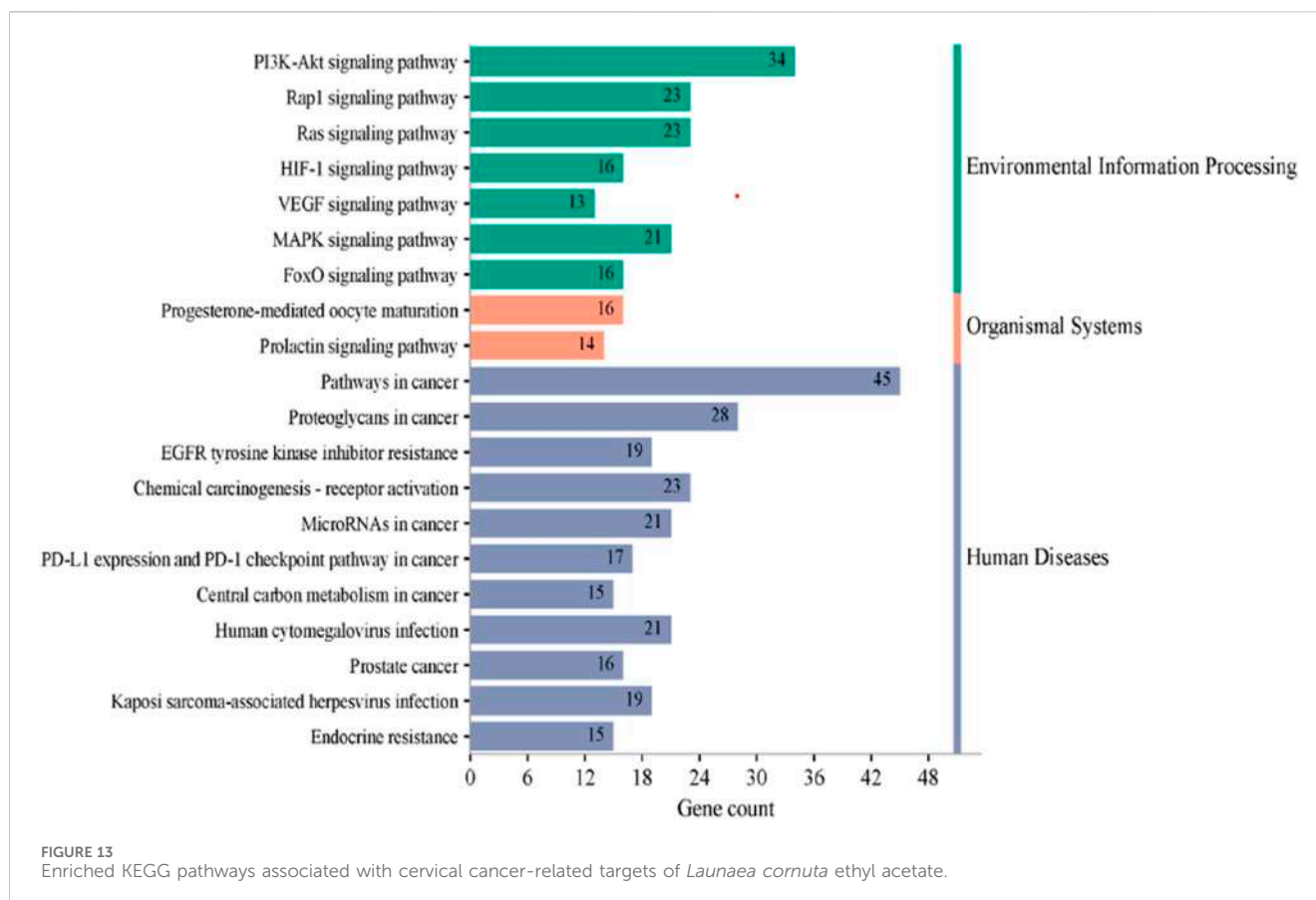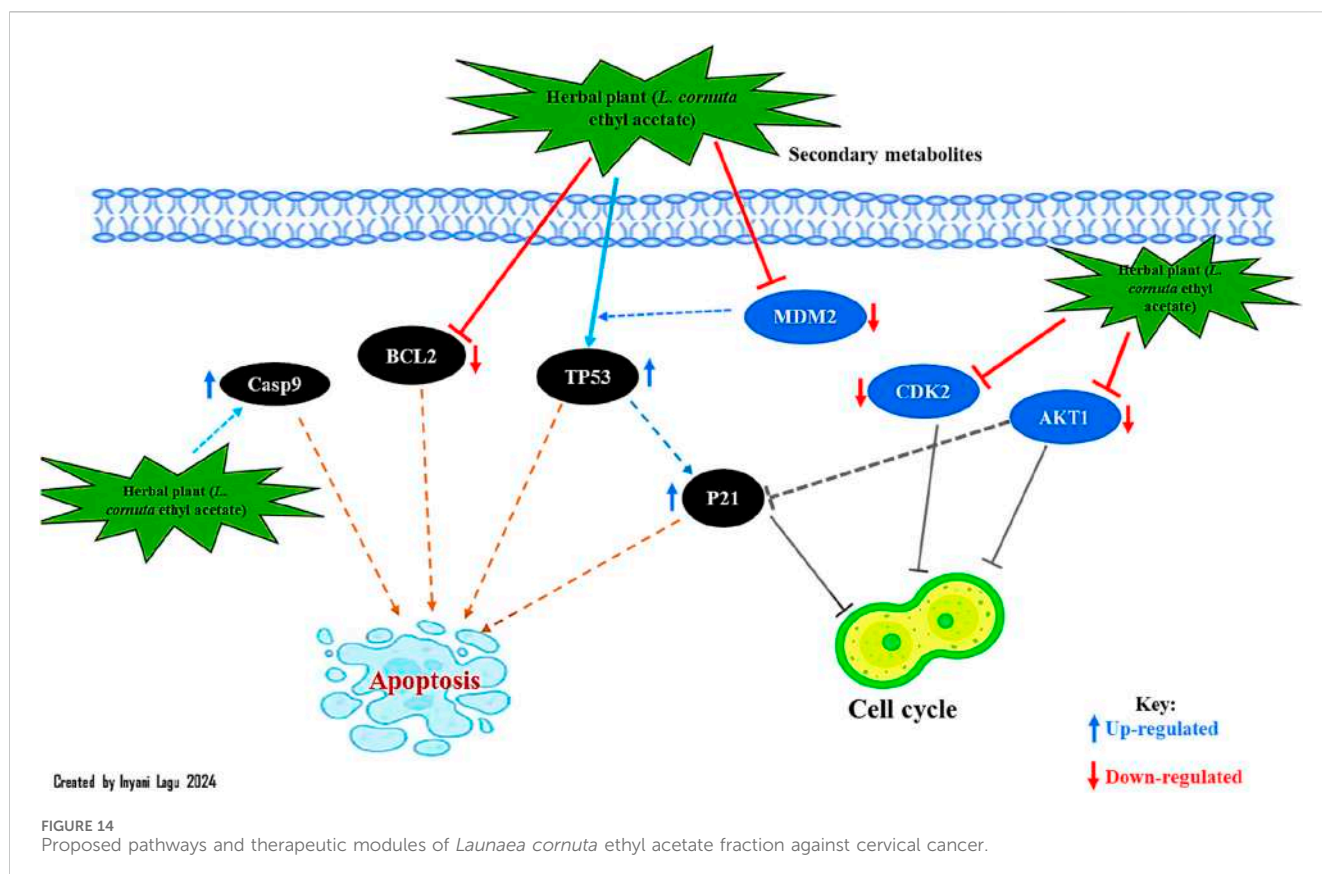
Discussion

Cervical cancer, among other cancers, remains one of the leading causes of mortality in women worldwide (Cohen et al., 2019; Kasi et al., 2021). Due to the increased global prevalence of cervical cancer and its poor prognosis, cervical cancer remains undetected in the early stages, resulting in patients with advanced stages; also, due to emerging drug resistance in cervical cancer treatment, there is a need for alternative drug design and development that involves target-specific therapies (Xi et al., 2023). Regardless of some drugs such as cisplatin, paclitaxel (Taxol), and carboplatin approved and recognised by the FDA of the United States, they tend to have adverse effects and resistance in patients with cervical cancer (Li et al., 2016). Furthermore, there are limited effective treatments for advanced cervical cancer. However, the high cost of cancer treatment is a significant constraint on patients' access to quality healthcare in low-income countries. These populations tend to prefer traditional herbs that are relatively affordable and available. Research shows that natural products from medicinal herbs are increasingly valuable in developing anticancer drugs (Elshamy et al., 2019; Owolabi et al., 2020). In this regard, *L. cornuta* merits our attention because it has been widely used as a traditional medicine among Kenyan communities to treat various diseases, including cancers (Ibrahim, 2021; Chemweno et al., 2022).

Using MTT assay, we evaluated the antiproliferative activity of the crude extract, hexane, ethyl acetate and water fractions from aerial parts of *L. cornuta* against cervical cancer cell lines. Our results demonstrated selective antiproliferative effect of *L. cornuta* ethyl acetate fraction by inhibiting cellular proliferation in cervical cancer cells (HeLa-229) by less than 50% cell viability. The dose-dependent cytotoxicity test showed

antiproliferative effects of *L. cornuta* ethyl acetate on HeLa cells in a dose-dependent manner with minimal cytotoxicity on non-cancerous cells. The ethyl acetate fraction of *L. cornuta* showed potent cytotoxic effects on HeLa cells as defined by the guidelines of the US National Cancer Institute (NCI), where an extract is generally considered to have *in vitro* cytotoxic activity if the IC_{50} value is ≤ 30 μg/mL after 48 h of incubation (Ogbole et al., 2017; Okpako et al., 2023b). We observed that the *L. cornuta* ethyl acetate fraction exhibited cytotoxicity on HeLa cells with an IC_{50} value of 20.56 μg/mL, thus presenting *L. cornuta* ethyl acetate fraction as a potential chemotherapeutic drug agent for cervical cancer. Previous studies reported the biological activity of *Launaea* species against various types of cancer cell lines, such as breast cancer, MCF-7, A549, and HCC cell lines (Rawat et al., 2016; Rezaei Seresht et al., 2016; Abouzied et al., 2021). Notably, this study is the first to report the anticancer activity of *L. cornuta* against HeLa cell line. On the other hand, *L. cornuta* ethyl acetate fraction did not display toxicity toward normal cells (An IC_{50} of 48.83 μg/mL), setting a safety margin (selectivity index) of 2.38, which agreed with the safety margin threshold for drugs. A selectivity index greater than 2 is considered highly selective (Canga et al., 2022). Therefore, the anticancer activity exhibited by *L. cornuta* ethyl acetate fraction was not a result of general cellular toxicity compared with the doxorubicin, having a selective index of 1.64. Furthermore, *L. cornuta* ethyl acetate fraction demonstrated a substantial inhibitory effect on HeLa cell migration. It was noted that the wound size remained relatively open by almost 50% relative migration distance in HeLa cells treated with *L. cornuta* ethyl acetate fraction compared with the untreated cells. This result is consistent with findings from Khan *et al.* (2024) and Lin *et al.* (2022), where 6-gingerol and puerarin exhibited antimigration effects by

FIGURE 14
Proposed pathways and therapeutic modules of *Launaea cornuta* ethyl acetate fraction against cervical cancer.
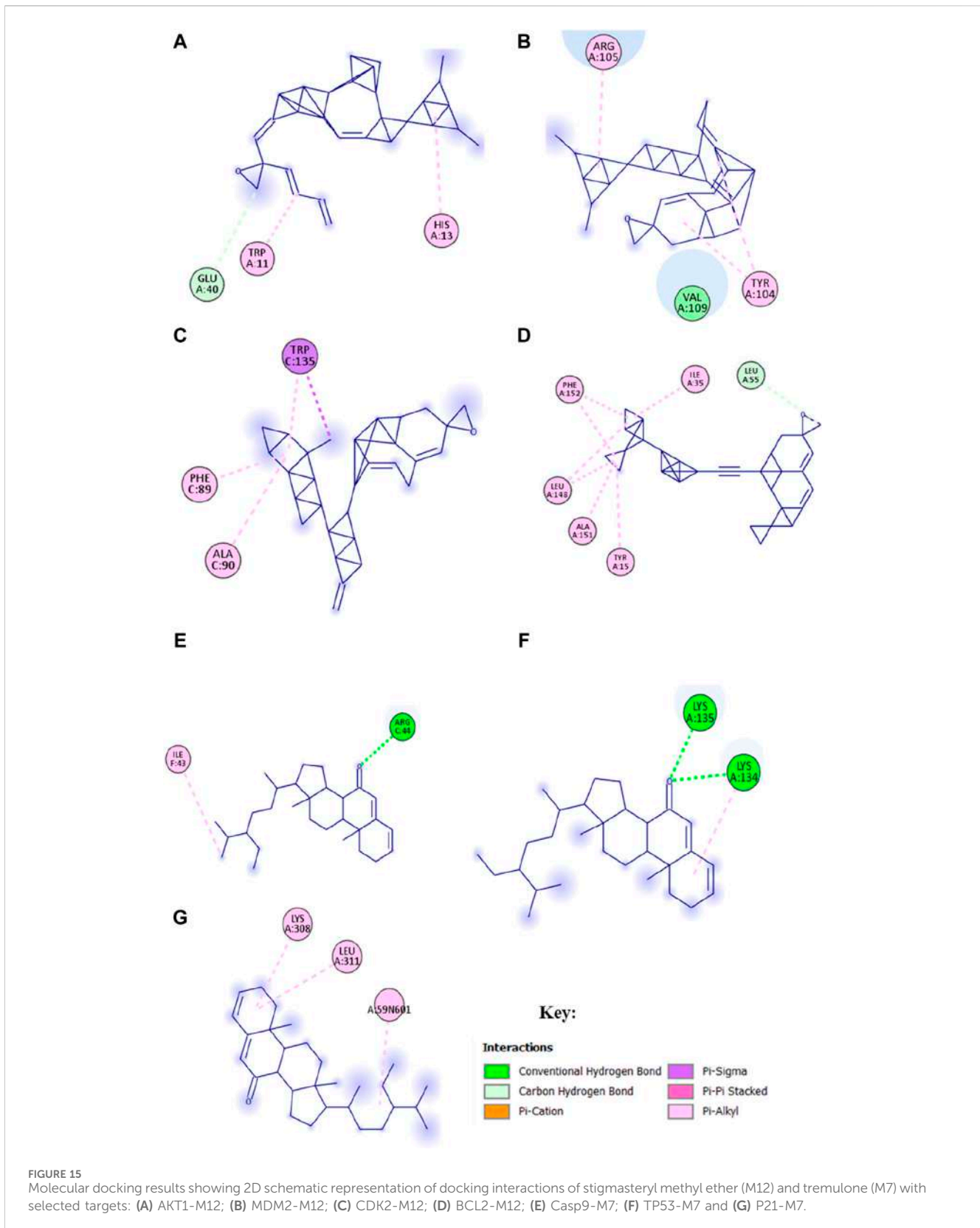
suppressing the migration of PC-3 cancer cells and Ishikawa endometrial cancer cells, respectively (Lin et al., 2022; Khan et al., 2024). Thus, justifying the extract's ability to prevent cancer cell metastases. Furthermore, we also studied the morphological changes in HeLa cells exposed to varying concentrations of the *L. cornuta* ethyl acetate fraction for 48 h. The data showed that *L. cornuta* ethyl acetate fraction triggered morphological changes in cells, including diminished HeLa cell viability with irregular and rounded shapes, detached from each other in a dose-dependent as compared with untreated HeLa cells, which remain in an organised monolayer with regular shapes. This finding tallied with the study reported by Ghosh *et al.* (2020) noted the atypical morphological changes of HeLa cells exposed to *Hexagonia glabra* after 24 h (Ghosh et al., 2020). In summary, these findings indicate the potential effects of *L. cornuta* ethyl acetate fraction in inhibiting proliferation in HeLa cells.

The preliminary screening of *L. cornuta* showed the presence of phenols, glycosides, tannins, and terpenoids in the ethyl acetate fraction of *L. cornuta*, which were also reported by previous findings in *L. cornuta* ethyl acetate aerial extract (Akimat et al., 2021; Maina et al., 2022). Thirteen (13) photochemical compounds were identified in *L. cornuta* ethyl acetate fraction through GC-MS analysis, and fatty acids and terpenoids were the most abundant compounds. These compounds were not similar to those reported by Machocho *et al.* (2014) in the aerial extract of *L. cornuta* ethyl acetate (Machocho et al., 2014). Some of the compounds identified in *L. cornuta* ethyl acetate fraction have been previously reported to exhibit anticancer (cytotoxic and antioxidant) activity against various cancer cell lines; these included ethyl (9Z,12Z,15Z)-octadeca-9,12,15-trienoate (fatty acids) (Chumkaew et al., 2014; Eid et al., 2021; Huang et al., 2022), Stigmast-5-ene, 3beta-methoxy- (phytosterols) (Chumkaew et al., 2014; Alvarez-sala

et al., 2019; Jaiganesh et al.) and tremulone (terpenoids) (Gupta and Chaphalkar, 2016; Lehtonen and Kaarniranta, 2016). These compounds were reported to induce cytotoxic effects in cancer cells through at least one of the pathways: apoptosis, inhibition of cell cycle, invasion and metastasis (Shaikhaldein et al., 2022). However, some of the compounds identified in our study have not been reported to exhibit anticancer activity, and their presence in the ethyl acetate fraction of *L. cornuta* may suggest that they work synergistically with other compounds (Ibrahim et al., 2022). Given the presence of these compounds in *L. cornuta*, ethyl acetate fraction could be attributed to the cytotoxic effects of the plants on cervical cancer cells. However, further research should be done to evaluate the anticancer activity of these individual compounds identified in the ethyl acetate fraction of *L. cornuta*.

The Gene Ontology and Kyoto Encyclopaedia of Genes and Genome Analysis presented several pathways as well as other diseases and disorders for the top hub genes. GO enrichment analysis revealed the direct involvement of the identified compounds in the regulation or progression of cervical cancer through programmed cell death, cell population, apoptotic processes, positive regulation of molecular function, and mitogen-activated protein (MAP) signalling. The KEGG pathway analysis showed that PI3K-AKT1 signalling was a significantly enriched pathway for *L. cornuta* ethyl acetate compounds. The EGFR tyrosine kinase inhibitor pathway, the MAPK signalling pathway, the Ras signalling pathway, and the FoxO signalling pathway were also enriched, suggesting the use of *L. cornuta* ethyl acetate fraction in the development of multi-target drugs. The MAPK pathway is known to play a role in inducing apoptosis and cell cycle arrest in tumorigenic cells (Chen, 2020; Huang et al.,

FIGURE 15
Molecular docking results showing 2D schematic representation of docking interactions of stigmasteryl methyl ether (M12) and tremulone (M7) with selected targets: **(A)** AKT1-M12; **(B)** MDM2-M12; **(C)** CDK2-M12; **(D)** BCL2-M12; **(E)** Casp9-M7; **(F)** TP53-M7 and **(G)** P21-M7.

2020; Tatekawa et al., 2024). Adding to the evidence from the pathway enrichment for *L. cornuta* ethyl acetate, the plant extracts may be used in targeting prostate cancer, human

cytomegalovirus infection, and endocrine resistance treatment. PI3K/Akt pathway is known to play a key role in cancer cell proliferation, metastasis, differentiation, and drug resistance (Xia
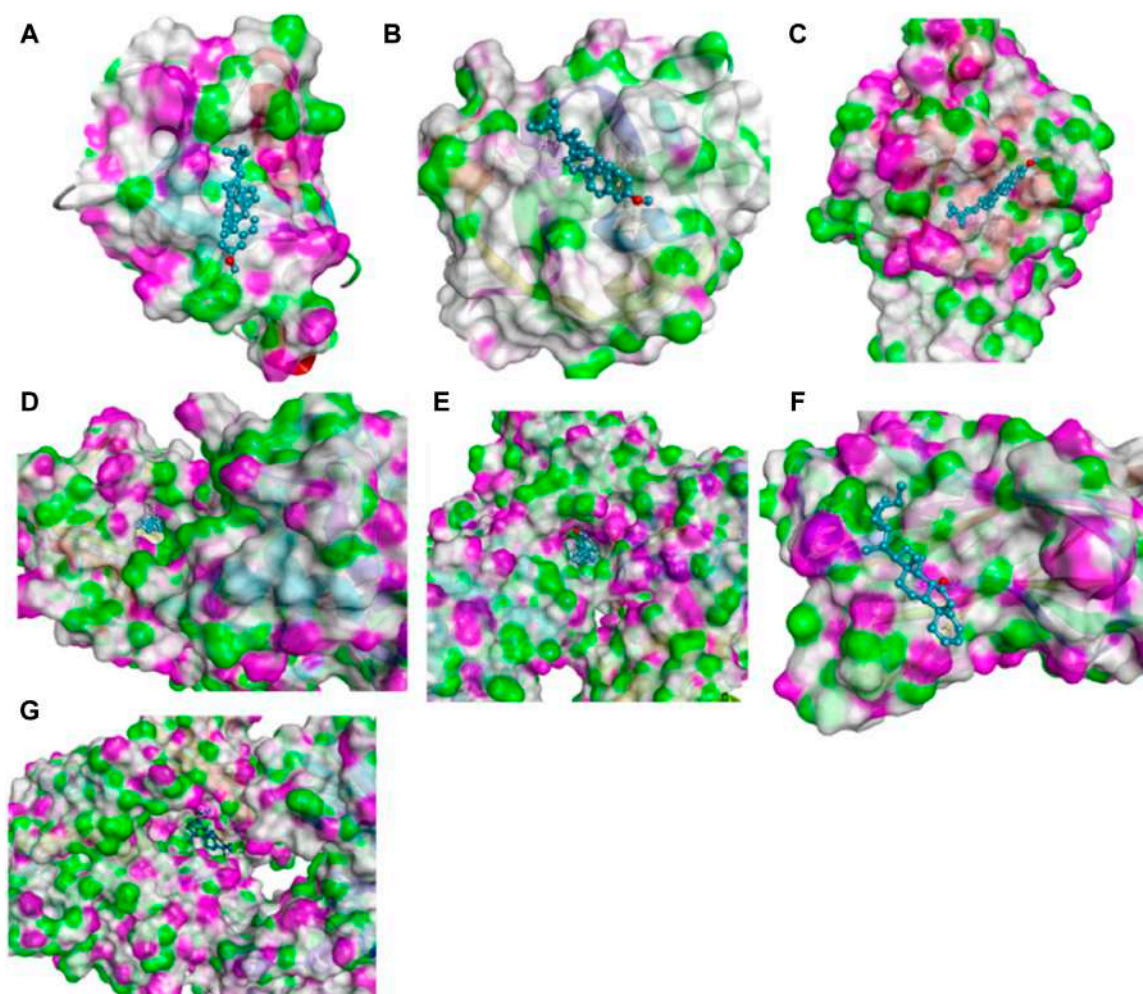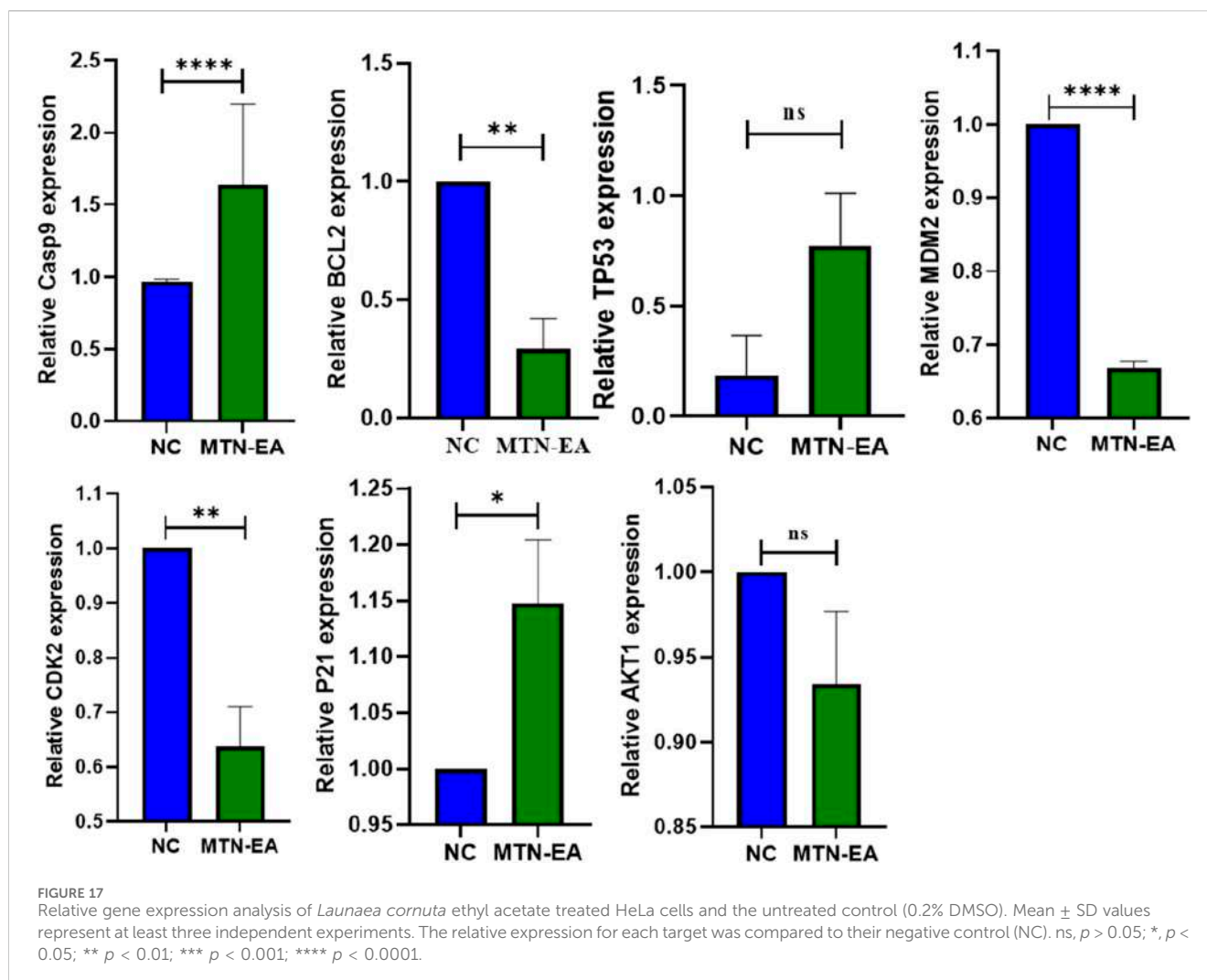
FIGURE 16
Molecular docking results showing 3D schematic presentation of M12 and M7 with target genes **(A)** AKT1-M12, **(B)** MDM2-M12, **(C)** CDK2-M12, **(D)** BCL2-M12, **(E)** Casp9-M7, **(F)** TP53-M7 and **(G)** P21-M7).

et al., 2015; Arjumand et al., 2016). Previous studies have shown that activation of PI3K through Akt phosphorylation results in the regulation of cell proliferation, thus promoting tumour growth (Arjumand et al., 2016; Jiang et al., 2020; Ma et al., 2024). Potential drug-like compounds that can inhibit cancer cell progression by negatively inhibiting Akt phosphorylation and downregulation of Akt kinase, thus regulating the PI3K-Akt pathway, could be a potential anticancer drug (Tao et al., 2017; Mart et al., 2023). Therefore, targeting the PI3K/Akt signalling pathway and its downstream targets, such as STAT3 and mTOR, may be a therapeutic option for *L. cornuta* ethyl acetate.

To validate the results of the network analysis, molecular docking was performed. As shown by molecular docking results, *L. cornuta* ethyl acetate' stigmasteryl methyl ether (M12) and tremulone (M7) exhibited good interaction toward AKT1, CDK2, MDM2, BCL2, TP53, P21, and Casp9 proteins with binding affinity ranging from −7.0 to −12.6 kcal/mol. A docking score of less than −5 kcal/mol has been shown to represent a good binding affinity (Zhao et al., 2022), which means that the lower the docking score, the more stable and stronger the affinity between compounds and targets. As shown by the docking scores, the binding

energies of all docking were less than −7.0 kcal/mol, indicating that these target genes have good and stable binding affinity with stigmasteryl methyl ester and tremulone compounds, respectively. Moreover, the binding energy values of the compounds docked with the selected target proteins are lower than those of the native ligands redocked with the selected proteins. Therefore, these results implies that M7 and M12 compounds exhibited good binding affinity and can form more stable interactions with the targeted proteins in cervical cancer cells. M7 and M12 compounds bonds to the CDK2, BCL2, Casp9 and P21 proteins through the same active binding pocket implicated in the binding of the native co-recrystallised ligands, suggesting M7 and M12 compounds maybe orthosteric hits. Whereas, M7 and M12 interacted with AKT1, MDM2, and TP53 proteins through different hydrogen and hydrophobic interacting amino acid residues (active binding pocket), which are not implicated in the binding of the native co-recrystallised ligand of redocked, thus suggesting that M7 and M12 compounds could be an allosteric hit toward AKT1, MDM2 and TP53 proteins. The presence of hydrogen bonds, hydrophobic interactions, and van der Waals forces in the ligand-protein interactions are critical for protein-ligand stability. Hydrogen bonds

FIGURE 17
Relative gene expression analysis of *Launaea cornuta* ethyl acetate treated HeLa cells and the untreated control (0.2% DMSO). Mean $\pm$ SD values represent at least three independent experiments. The relative expression for each target was compared to their negative control (NC). ns, $p > 0.05$; *, $p < 0.05$; ** $p < 0.01$; *** $p < 0.001$; **** $p < 0.0001$.

improve specificity, hydrophobic interactions augment the drug effects, and van der Waals forces improve structural fit between molecules, resulting in increased drug efficacy and potency in therapeutic applications (Dhar and Roy, 2020; Nussinov et al., 2023).

The gene expression levels of P21 and Casp9 were found to be high in HeLa cells treated with the ethyl acetate fraction *of L. cornuta* (20.56 μg/mL) compared to the untreated control. Studies by Dalghi *et al.* (2023), and Zhou *et al.* (2024) reported that high expression levels of P21 in cancer cells are implicated in the promotion of cell cycle arrest and apoptosis (Dalghi et al., 2023; Zhou et al., 2024). BCL2 is a known inhibitor of apoptosis (Babakanrad et al., 2023; Branch et al., 2023; Hosseini et al., 2024). Cancer cells typically evade cell death by upregulating antiapoptotic proteins like BCL-2 or inhibiting pro-apoptotic proteins such as Casp9. BCL-2 inhibits mitochondrial apoptosis by binding to pro-apoptotic proteins and blocking pore formation and cytochrome *c* release. Caspases and upstream regulatory factors, such as p53, trigger apoptosis (Ghosh et al., 2020). As observed in our results, there was downregulation of BCL2 with concomitant upregulation of caspase-9 in HeLa cells treated with *L. cornuta* ethyl acetate compared to the untreated HeLa cells; this pattern was also reported by Eltamany *et al.* (2022). MDM2 is a protein that directly regulates TP53 function and stability (Hou et al., 2019; Zhu et al., 2021); as noted in this study, MDM2 was significantly down- regulated ($p < 0.0001$) and therefore, the expression

level of TP53 was insignificantly expressed ($p > 0.05$) in treated HeLa cells compared to the untreated control. Study by Zhu *et al.* (2021) reported that downregulation of the expression level of MDM2 results in upregulation of TP53 expression, resulting in the induction of cell cycle arrest and apoptosis in cervical cancer cells (Zhu et al., 2021). CDK is well known to regulate the transition of the cell cycle from the G1 phase to the S phase, thus accelerating the S phase and the proliferation efficiency in cells. It is highly expressed in cancer cells (Liu et al., 2013; Tadesse et al., 2020; Bao et al., 2023). *L. cornuta* ethyl acetate fraction elicited a significant downregulation of CDK2 ($p > 0.01$), which is consistent with the study reported by Zhong *et al.* (2019) (Zhong et al., 2019). Therefore, the downregulation of CDK2 in HeLa cells could be attributed to the anticancer effect of the *L. cornuta* ethyl acetate fraction through suppression of the cell cycle. Furthermore, the expression level of AKT was observed to be insignificant in treated HeLa cells despite its crucial role in the regulation of cell survival, angiogenesis, and tumorigenesis of cancer (Rashmi et al., 2014).

Conclusion

The *L. cornuta* ethyl acetate fraction demonstrates significant antiproliferative effects against cervical cancer HeLa cells, with

minimal cytotoxicity on non-cancerous cells and rich composition of fatty acids and terpenoids identified through GC-MS analysis. Network analysis has pinpointed drug-like compounds, including 2-linoleolglycerol, tremulone, spiro [2.5] non-4-ene, 4-ethyl-8-methylene-5-trimethylsilyl, ethyl (9Z, 12Z, 15Z)-octadeca-9,12,15-trienoate, stigmasteryl methyl ether and tricylo [20.8.0.0 (7,16)] triacontane, 1(22),7(16)-diepoxy targeting key proteins involved in cancer progressions and tumorigenesis, such as AKT2, MDM STAT3, EGFR, CDK2, MTOR, MAPK3a PTGS2, MCL1 and TNF among others. Intriguingly, the gene expression levels of BCL2, CDK2, MDM2, Casp9 and P21 were reversed in HeLa cells treated with *L. cornuta* ethyl acetate fraction when compared with the untreated HeLa cells, indicating its potential to regulate cell proliferation, apoptosis, and cell cycle in cancer cells. These findings highlight *L. cornuta's* promise as a multi-target anticancer drug, warranting further *in-vitro* and *in vivo* studies to assess its efficacy and safety for clinical use as well as anticancer activity on other cancer cell lines.

Data availability statement

The datasets presented in this study can be found in online repositories. The names of the repository/repositories and accession number(s) can be found in the article/Supplementary Material.

Ethics statement

Ethical approval was not required for the studies on humans in accordance with the local legislation and institutional requirements because only commercially available established cell lines were used. Ethical approval was not required for the studies on animals in accordance with the local legislation and institutional requirements because only commercially available established cell lines were used.

Author contributions

IL: Conceptualization, Data curation, Formal Analysis, Funding acquisition, Investigation, Methodology, Resources, Software, Validation, Visualization, Writing–original draft, Writing–review and editing. DN: Conceptualization, Methodology, Supervision, Writing–review and editing. SN: Conceptualization, Funding acquisition, Methodology, Resources, Supervision, Writing–review and editing.

Conflict of interest

The authors declare that the research was conducted in the absence of any commercial or financial relationships that could be construed as a potential conflict of interest.

Publisher's note

All claims expressed in this article are solely those of the authors and do not necessarily represent those of their affiliated organizations, or those of the publisher, the editors and the reviewers. Any product that may be evaluated in this article, or claim that may be made by its manufacturer, is not guaranteed or endorsed by the publisher.

Supplementary material

The Supplementary Material for this article can be found online at: https://www.frontiersin.org/articles/10.3389/fphar.2024.1399885/full#supplementary-material

References

Abouzied, A. S., Break, M. K. B., Younes, K. M., Ads, E. N., Syed, R. U., Alafnan, D., et al. (2021). *In vitro* antimicrobial, anticancer, and apoptosis-inducing effects of the methanolic extract of Launaea mucronata. *Not. Bot. Horti Agrobot. Cluj-Napoca* 49 (4), 12556–12614. doi:10.15835/nbha49412556

Ahmed Khan, D., Shahid, A., Sherif, A. E., Aati, H. Y., Abdullah, M., Mehmood, K., et al. (2023). A detailed biochemical characterization, toxicological assessment and molecular docking studies of Launaea fragilis: an important medicinal xero-halophyte. *Saudi Pharm. J.* 31 (6), 1047–1060. doi:10.1016/j.jsps.2023.04.028

Akimat, E. K., Omwenga, G. I., Moriasi, G. A., and Ngugi, M. P. (2021). Antioxidant, anti-inflammatory, acute oral toxicity, and qualitative phytochemistry of the aqueous root extract of launaea cornuta (hochst. Ex Oliv. & hiern.). *J. Evidence-Based Integr. Med.* 26, 2515690X211064585. doi:10.1177/2515690X211064585

Alvarez-sala, A., Attanzio, A., Tesoriere, L., Barberá, R., and Cilla, A. (2019). Apoptotic effect of a phytosterol-ingredient and its main phytosterol (β-sitosterol) in human cancer cell lines. *Int. J. Food Sci. Nutr.* 70 (3), 323–334. doi:10.1080/09637486.2018.1511689

Arjumand, W., Merry, C. D., Wang, C., Saba, E., McIntyre, J. B., Fang, S., et al. (2016). Phosphatidyl inositol-3 kinase (PIK3CA) E545K mutation confers cisplatin resistance and a migratory phenotype in cervical cancer cells. *Oncotarget* 7 (50), 82424–82439. doi:10.18632/oncotarget.10955

Babakanrad, E., Mohammadian, T., Esmaeili, D., and Behzadi, P. (2023). Studying the effect of gene fusion of A and C types capsular synthesizing enzymes and anticancer sequence on inducing the expression of apoptotic BCL-2, BAX, and Caspase-3 genes by Real-time RT-PCR method. *Heliyon* 9 (5), e16326. doi:10.1016/j.heliyon.2023.e16326

Balasubramaniam, S. D., Balakrishnan, V., Oon, C. E., and Kaur, G. (2019). Key molecular events in cervical cancer development. *Med* 55 (7), 384. doi:10.3390/medicina55070384

Bao, X. J., Wenli, L., Sun, T., Wang, J. W., Liu, X. F., Li, M. X., et al. (2023). Clinical data analysis of cdks expression and prognosis in breast cancer. *World Cancer Res. J.* 10, 1–15. doi:10.32113/wcrj_20231_2475

Black, E., and Richmond, R. (2018). Prevention of cervical cancer in sub-saharan Africa: the advantages and challenges of HPV vaccination. *Vaccines* 6 (3), 61. doi:10.3390/vaccines6030061

Branch, N. T., Sepahy, A. A., Branch, N. T., and Torbati, M. B. (2023). Investigating the synergism of. 12(48):51–64.

Canga, I., Vita, P., Oliveira, A. I., Castro, M. Á., and Pinho, C. (2022). *In vitro* cytotoxic activity of african plants: a review. *Molecules* 27 (15), 4989–5018. doi:10.3390/molecules27154989

Chemweno, T., Mwamburi, L., and Keter, L. (2022). Evaluation of the antibacterial activity of Launaea cornuta extracts. *Res. Sq. Platf.*, 1–11. Published online. doi:10.21203/rs.3.rs-1829910/v1

Chen, H. (2020). Downregulation of SEMA4C inhibit epithelial- mesenchymal transition (EMT) and the invasion and metastasis of cervical cancer cells via inhibiting transforming growth factor-beta 1 activated protein kinase (MAPK) activation. Published online 1–11. doi:10.12659/MSM.918123

Chumkaew, P., Kato, S., and Chantrapromma, K. (2014). Journal of asian natural products new cytotoxic steroids from the fruits of syzygium siamense. 37–41. doi:10.1080/10286021003762028

Cohen, P. A., Jhingran, A., Oaknin, A., and Denny, L. (2019). Cervical cancer. *Lancet* 393 (10167), 169–182. doi:10.1016/S0140-6736(18)32470-X

Daina, A., Michielin, O., and Zoete, V. (2019). SwissTargetPrediction: updated data and new features for efficient prediction of protein targets of small molecules. *molecules* 47 (May), 357–364. doi:10.1093/nar/gkz382

Dalghi, E., Khajavi, A. F., and Ahmadi, R. (2023). *The effect of aspirin on caspase-8 and -9 activity level in cervical cancer cells in vitro*, 2–11. Published online.

Dhar, P., and Roy, P. (2020). Molecular docking unmasks potent phytoligands against sars-cov-2 spike glycoprotein, main protease, papain-like protease, and RNA-dependent RNA polymerase. *Def. Life Sci. J.* 5 (4), 255–267. doi:10.14429/dlsj.5.15999

Drokow, E. K., Fangninou, F. F., Effah, C. Y., Agboyibor, C., Zhang, Y., Arboh, F., et al. (2022). Cervical cancer survival times in Africa. *Front. Public Heal* 10, 981383. doi:10.3389/fpubh.2022.981383

Eid, M. S. A. hwaiti, Ghassan, M. A., Sheikha, A., Bakchiche, B., Pham, T. H., Thomas, R. H., et al. (2021). Evaluation of the anticancer activity and fatty acids composition of " Handal " (*Citrullus colocynthis* L.) seed oil, a desert plant from south Jordan. *Food Sci. Nutr.* 9, 282–289. doi:10.1002/fsn3.1994

Elshamy, A. I., Abd-ElGawad, A. M., El-Amier, Y. A., El, G.AENG, and Al-Rowaily, S. L. (2019). Interspecific variation, antioxidant and allelopathic activity of the essential oil from three Launaea species growing naturally in heterogeneous habitats in Egypt. *Flavour Fragr. J.* 34 (5), 316–328. doi:10.1002/ffj.3512

Fatuma Some, G. K. (2014). Ethnomedicinal plants traditionally used by the keiyo community in elgeyo marakwet county, Kenya. *J. Biodivers. Bioprospecting Dev.* 01 (03), 1–11. doi:10.4172/2376-0214.1000132

Ghosh, S. K., Sanyal, T., and Bera, T. (2020). Anticancer activity of solvent extracts of Hexogonia glabra against cervical cancer cell lines. *Asian Pac. J. Cancer Prev.* 21 (7), 1977–1986. doi:10.31557/APJCP.2020.21.7.1977

Gupta, A., and Chaphalkar, S. R. (2016). Terpenoids from three medicinal plants and their potential anti-inflammatory and immunosuppressive activity on human whole blood and peripheral blood. *Asian J. Ethnopharmacol. Med. Foods* 02 (1), 13–17.

Hosseini, E. S., Hoseini, S. M., Hasanshahi, G., Fatemeh, B., Sheikhha, M. H., and Montazeri, F. (2024). Comparing the effects of free and liposomal indole compounds on bax and Bcl2 gene expression changes in the KG-1 cell line. 14(1):53. doi:10.18502/ijpho.v14i1.14664

Hou, H., Sun, D., and Zhang, X. (2019). The role of MDM2 amplification and overexpression in therapeutic resistance of malignant tumors. *Cancer Cell Int.* 19 (1), 216–16. doi:10.1186/s12935-019-0937-4

Huang, W., Guo, X., Wang, C., Alzhan, A., Liu, Z., Ma, X., et al. (2022). α -Linolenic acid induces apoptosis, inhibits the invasion and metastasis, and arrests cell cycle in human breast cancer cells by inhibiting fatty acid synthase. *J. Funct. Foods* 92 (March), 105041. doi:10.1016/j.jff.2022.105041

Huang, X. bin, Jing, S. K., Bin, C. G., Liu, R., Jiang, Z. F., and He, Y. L. (2020). Circular RNA hsa _ circ _ 0003204 promotes cervical cancer cell proliferation, migration, and invasion by regulating MAPK pathway. *Cancer Biol. Ther.* 21 (10), 972–982. doi:10.1080/15384047.2020.1824513

Ibrahim, F. (2021). Total flavonoid content and antioxidant activity of launaea Cornuta leaf methanol and aqueous extracts. Published online.

Ibrahim, M., Kumar, R. K., and Fahim Mohammad, N. S. M. (2022). Natural Resources for human health. *Natr Resour. Hum. Heal.* (38960), 1–8. doi:10.53365/nrfhh/154598

Jaiganesh, S., Singaravelu, A., Shilpa, K., Lakshmi, J., Balakrishnan, A., Sujatha, S., et al. (2010). Biological evaluation of (3β)-STIGMAST-5-EN-3-OL as potent anti-diabetic agent in regulating glucose transport using *in vitro* model. *Int. J. Diabetes Mellitus* 2, 101–109. doi:10.1016/j.ijdm.2009.12.013

Jayawardena, T. U., Kim, H. S., Sanjeewa, K. K. A., Kim, S. Y., Rho, J. R., Jee, Y., et al. (2019). Sargassum horneri and isolated 6-hydroxy-4,4,7a-trimethyl-5,6,7,7a-tetrahydrobenzofuran-2(4H)-one (HTT); LPS-induced inflammation attenuation via suppressing NF-κB, MAPK and oxidative stress through Nrf2/HO-1 pathways in RAW 264.7 macrophages. *Algal Res.* 40 (January), 101513. doi:10.1016/j.algal.2019.101513

Jeddi, M., El, N., El, M., Benkhaira, N., Al-Mijalli, S. H., Kandsi, F., et al. (2023). Antimicrobial, antioxidant, α-amylase and α-glucosidase inhibitory activities of a chemically characterized essential oil from Lavandula angustifolia Mill., *in vitro* and *in silico* investigations. *vitro silico investigations* 111 (August), 104731. doi:10.1016/j.bse.2023.104731

Jiang, N., Dai, Q., Su, X., Fu, J., Feng, X., and Peng, J. (2020). Role of PI3K/AKT pathway in cancer: the framework of malignant behavior. *Mol. Biol. Rep.* 47, 4587–4629. doi:10.1007/s11033-020-05435-1

J, M., G, K. J., M, K. W., and M, M. J. (2015). Phytochemical screening and cytotoxicity evaluation of Launaea Cornuta H. (Asteraceae) using brine shrimp. *Merit Res. J. Med. Med. Sci.* 3 (4), 116–120.

Johnson, S. B., Park, H. S., Gross, C. P., and Yu, J. B. (2018). Complementary medicine, refusal of conventional cancer therapy, and survival among patients with curable cancers. *JAMA Oncol.* 4 (10), 1375–1381. doi:10.1001/jamaoncol.2018.2487

Juwitaningsih, T., Roza, D., Silaban, S., Hermawati, E., and Windayani, N. (2022). Phytochemical screening, antibacterial, antioxidant, and anticancer activity of Coffee parasite acetone extract (Loranthus ferrugineus Roxb). *Pharmacia* 69, 1041–1046. doi:10.3897/pharmacia.69.e91427

Kasi, D., R, A. H., Putankar, P. R., and Humera Sayeeda Mbbs, N. (2021). Cervical cancer: an overview. *IOSR J. Dent. Med. Sci. e-ISSN* 20 (5), 11–21. doi:10.9790/0853-2005101121

Khan, H., Azad, I., Arif, Z., Parveen, S., Kumar, S., Rais, J., et al. (2024). Structure based docking and biological evaluation towards exploring potential anti-cancerous and apoptotic activity of 6-Gingerol against human prostate carcinoma cells. *BMC Complement. Med. Ther.* 24 (1), 8–23. doi:10.1186/s12906-023-04269-1

Khan, Z., Iqbal, M., Ahmed, W., Khayam, M., Kiran, S., Subhan, A., et al. (2016). *In vitro* haemolytic and thrombolytic activities of Launaea cornuta. *Asian J. Chem.* 28 (5), 1084–1086. doi:10.14233/ajchem.2016.19591

Lehtonen, M., and Kaarniranta, K. (2016). Terpenoids: natural inhibitors of NF- κ B signaling with anti-inflammatory and anticancer potential Review Terpenoids: natural inhibitors of NF- k B signaling with anti-inflammatory and anticancer potential. doi:10.1007/s00018-008-8103-5

Li, F., Li, K., Li, D., Zhang, W., Yang, K. W., Ke, D., et al. (2023). ATG10 overexpression is related to the dismal prognosis and promotes the growth and migration of hepatocellular carcinoma cells via cyclin B1/CDK1 and CDK2. *Am. J. Cancer Res.* 13 (4), 1188–1208.

Li, H., Wu, X., and Cheng, X. (2016). Advances in diagnosis and treatment of metastatic cervical cancer. *J. Gynecol. Oncol.* 27 (4), e43. doi:10.3802/jgo.2016.27.e43

Li, M., and Ren, C. (2022). Exploring the protective mechanism of baicalin in treatment of atherosclerosis using endothelial cells deregulation model and network pharmacology. *BMC Complement. Med. Ther.* 22 (1), 257. doi:10.1186/s12906-022-03738-3

Lin, Z., Sui, X., Jiao, W., Wang, Y., and Zhao, J. (2022). Exploring the mechanism and experimental verification of puerarin in the treatment of endometrial carcinoma based on network pharmacology and bioinformatics analysis. *BMC Complement. Med. Ther.* 22 (1), 150. doi:10.1186/s12906-022-03623-z

Liu, T., Liu, Y., Bao, X., Tian, J., Liu, Y., and Yang, X. (2013). Overexpression of TROP2 predicts poor prognosis of patients with cervical cancer and promotes the proliferation and invasion of cervical cancer cells by regulating. *ERK Signal. Pathw.* 8 (9), 1–14. doi:10.1371/journal.pone.0075864

Lu, J. jian, Dang, Y. ye, Huang, M., Xu, W. shan, Chen, X. ping, and Wang, Y. tao (2012). Anti-cancer properties of terpenoids isolated from Rhizoma Curcumae – a review. *J. Ethnopharmacol.* 143 (2), 406–411. doi:10.1016/j.jep.2012.07.009

Luo, X., Zhao, M., Liu, S., Zheng, Y., Zhang, Q., Bao, Y. R., et al. (2023). Effect of Oroxylum indicum on hepatocellular carcinoma via the P53 and VEGF pathways based on microfluidic chips. *BMC Complement. Med. Ther.* 23 (1), 400–418. doi:10.1186/s12906-023-04217-z

Ma, G., Dong, Q., Li, F., Jin, Z., Pi, J., Wu, W., et al. (2024). Network pharmacology and *in vivo* evidence of the pharmacological mechanism of geniposide in the treatment of atherosclerosis. *BMC Complement. Med. Ther.* 24 (1), 53–15. doi:10.1186/s12906-024-04356-x

Machocho, A., Karau, G., Njagi, E., Koech, L., and Wangai, L. (2014). Profiling of the chemical compounds in ethyl acetate extracts of launaea cornuta asteraceae by gc-ms. *Int. J. Pharmacogn.* 1 (5), 296–300. doi:10.13040/IJPSR.0975-8232.1(5).296-00

Maina, M., Mbaria, J., Kamanja, I., and Moriasi, G. (2022). Acute oral toxicity, cognitive-enhancing and anti-lipid peroxidation efficacy, and qualitative phytochemistry of the aqueous aerial Part Extract of launaea cornuta (hochst. Ex. Oliv. &Hiern) C. Jeffrey. *SSRN Electron J.* 9 (4), e15487. doi:10.2139/ssrn.4297902

Mart, A., Romero, I. C., Amparan, L. C., Castañeda, J. R., and Ayala, G. (2023). The insulin receptor substrate 2 mediates the action of insulin on HeLa cell migration via the PI3K/Akt signaling pathway. *Curr. Issues Mol. Biol.* 45, 2296–2308. Published online. doi:10.3390/cimb45030148

Martínez-Rodríguez, F., Limones-González, J. E., Mendoza-Almanza, B., Esparza-Ibarra, E. L., Gallegos-Flores, P. I., Ayala-Luján, J. L., et al. (2021). Understanding cervical cancer through proteomics. *Cells* 10 (8), 1854–1925. doi:10.3390/cells10081854

Misonge, J. M., Wakori, E. W. T., Kimondo, J. N., Kisengi, J. M., Waiganjo, B. W., Mwambeo, M. H., et al. (2016). Assessment of diversity and conservation status of plants at mount Kenya university medicinal botanical garden, thika sub-county, kiambu county, Kenya. *Int. J. Biodivers. Conserv.* 8 (6), 120–125. doi:10.5897/ijbc2015.0891

Mongalo, N. I., McGaw, L. J., Finnie, J. F., and Van Staden, J. (2017). Pharmacological properties of extracts from six South African medicinal plants used to treat sexually transmitted infections (STIs) and related infections. *South Afr. J. Bot.* 112, 290–295. doi:10.1016/j.sajb.2017.05.031

Musila, M. F., Dossaji, S. F., Nguta, J. M., Lukhoba, C. W., and Munyao, J. M. (2013). *In vivo* antimalarial activity, toxicity and phytochemical screening of selected antimalarial plants. *J. Ethnopharmacol.* 146 (2), 557–561. doi:10.1016/j.jep.2013.01.023

Njeru, S. N., Kraus, J., Meena, J. K., Lechel, A., Katz, S. F., Kumar, M., et al. (2020). Aneuploidy-inducing gene knockdowns overlap with cancer mutations and identify Orp3 as a B-cell lymphoma suppressor. *Oncogene* 39 (7), 1445–1465. doi:10.1038/s41388-019-1073-2

Njeru, S. N., and Muema, J. M. (2020). Antimicrobial activity, phytochemical characterization and gas chromatography-mass spectrometry analysis of Aspilia pluriseta Schweinf. extracts. *Heliyon* 6 (10), e05195. doi:10.1016/j.heliyon.2020.e05195

Njeru, S. N., and Muema, J. M. (2021). *In vitro* cytotoxicity of Aspilia pluriseta Schweinf. extract fractions. *BMC Res. Notes* 14 (1), 57–7. doi:10.1186/s13104-021-05472-4

Njeru, S. N., Obonyo, M. A., Nyambati, S. O., and Ngari, S. M. (2015). Antimicrobial and cytotoxicity properties of the crude extracts and fractions of Premna resinosa (Hochst.) Schauer (Compositae): Kenyan traditional medicinal plant. *BMC Complement. Altern. Med.* 15 (1), 295–299. doi:10.1186/s12906-015-0811-4

Nussinov, R., Zhang, M., Liu, Y., and Jang, H. (2023). AlphaFold, allosteric, and orthosteric drug discovery: ways forward. *Drug Discov. Today* 28 (6), 103551. doi:10.1016/j.drudis.2023.103551

Ochwangi, D. O., Kimwele, C. N., Oduma, J. A., Gathumbi, P. K., Mbaria, J. M., and Kiama, S. G. (2014). Medicinal plants used in treatment and management of cancer in Kakamega County, Kenya. *J. Ethnopharmacol.* 151 (3), 1040–1055. doi:10.1016/j.jep.2013.11.051

Ogbole, O. O., Segun, P. A., and Adeniji, A. J. (2017). *In vitro* cytotoxic activity of medicinal plants from Nigeria ethnomedicine on Rhabdomyosarcoma cancer cell line and HPLC analysis of active extracts. *BMC Complement. Altern. Med.* 17, 494–510. Published online. doi:10.1186/s12906-017-2005-8

Okpako, I. O., Atieno, F., Kyama, C. M., Oyem, J. C., and Njeru, S. N. (2023a). Antiproliferative activity of Euphorbia ingens extract against prostate cancer cell line: an *in silico* and *in vitro* analysis. 1–20. doi:10.20944/preprints202305.1881.v1

Okpako, I. O., Ng'ong, a, F. A., Kyama, C. M., and Njeru, S. N. (2023b). Antiproliferative activity of ethyl acetate fraction of Euphorbia ingens against prostate cancer cell line: an *in silico* and *in vitro* analysis. *Sci. Afr.* 22 (October), e01943. doi:10.1016/j.sciaf.2023.e01943

Olthof, E. P., Wenzel, H. H. B., van der Velden, J., Stalpers, L. J. A., Mom, C. H., and van der Aa, M. A. (2024). Treatment strategies guided by [18F]FDG-PET/CT in patients with locally advanced cervical cancer and [18F]FDG-Positive lymph nodes. *Cancers (Basel)* 16 (4), 717. doi:10.3390/cancers16040717

Omara, T. (2020). Antimalarial plants used across Kenyan communities. *Evidence-based Complement. Altern. Med.* 2020, 4538602. doi:10.1155/2020/4538602

Omara, T., Odero, M. P., and Obakiro, S. B. (2022). Medicinal plants used for treating cancer in Kenya: an ethnopharmacological overview. *Bull. Natl. Res. Cent.* 46 (1), 148. doi:10.1186/s42269-022-00840-x

Onyancha, J. M., Gikonyo, N. K., Wachira, S. W., Mwitari, P. G., and Gicheru, M. M. (2018). Anticancer activities and safety evaluation of selected Kenyan plant extracts against breast cancer cell lines. *J. Pharmacogn. Phyther* 10 (2), 21–26. doi:10.5897/jpp2017.0465

Owolabi, M. S., Ogundajo, A. L., Alafia, A. O., Ajelara, K. O., and Setzer, W. N. (2020). Composition of the essential oil and insecticidal activity of launaea taraxacifolia (Willd.) Amin ex C. Jeffrey growing in Nigeria. *Foods* 9 (7), 914–918. doi:10.3390/foods9070914

Paken, J., Govender, C. D., Pillay, M., Feyasa, M., and Sewram, V. (2023). Cisplatin-associated ototoxicity amongst cervical cancer patients: a prospective cohort study in South Africa. *PLoS One* 18 (4 April), 02836399–e283721. doi:10.1371/journal.pone.0283639

Panyajai, P., Viriyaadhammaa, N., Tima, S., Chiampanichayakul, S., Dejkriengkraikul, P., Okonogi, S., et al. (2024). Anticancer activity of Curcuma aeroginosa essential oil and its nano-formulations: cytotoxicity, apoptosis and cell migration effects. *BMC Complement. Med. Ther.* 24 (1), 16–13. doi:10.1186/s12906-023-04261-9

Rashmi, R., DeSelm, C., Helms, C., Bowcock, A., Rogers, B. E., Rader, J. L., et al. (2014). AKT inhibitors promote cell death in cervical cancer through disruption of mTOR signaling and glucose uptake. *PLoS One* 9 (4), 929488–e93012. doi:10.1371/journal.pone.0092948

Rawat, P., Saroj, L. M., Kumar, A., Singh, T. D., Tewari, S. K., and Pal, M. (2016). Phytochemicals and cytotoxicity of Launaea procumbens on human cancer cell lines. *Pharmacogn. Mag.* 12 (47), S431–S435. doi:10.4103/0973-1296.191452

Revathidevi, S., Murugan, A. K., Nakaoka, H., Inoue, I., and Munirajan, A. K. (2021). APOBEC: a molecular driver in cervical cancer pathogenesis. *Cancer Lett.* 496 (October 2020), 104–116. doi:10.1016/j.canlet.2020.10.004

Rezaei Seresht, H., Aldaghi, L. S., Cheshomi, H., and Gholami, O. (2016). Phytochemical profile, antioxidant and cytotoxic activities of launaea acanthodes; an endemic species of Iran. *Int. J. Adv. Biotechnol. Res.*

Sanni, D. M., and Omotoyinbo, O. V. (2016). GC-MS analysis of pteleopsis suberosa stem bark methanol-chloroform extract. *J. Plant Sci.* 4 (3), 37. doi:10.11648/j.jps.20160403.11

Scatchard, K., Forrest, J. L., Flubacher, M., Cornes, P., and Williams, C. (2012). Chemotherapy for metastatic and recurrent cervical cancer. *Cochrane Database Syst. Rev.* 2012 (10), CD006469. doi:10.1002/14651858.CD006469.pub2

Sergazy, S., Vetrova, A., Orhan, I. E., Senol Deniz, F. S., Kahraman, A., Zhang, J. Y., et al. (2021). Antiproliferative and cytotoxic activity of Geraniaceae plant extracts against five tumor cell lines. *Future Sci. OA* 8. Published online. doi:10.2144/fsoa-2021-0109

Shaikh, J. R., and Patil, M. (2020). Qualitative tests for preliminary phytochemical screening: an overview. *Int. J. Chem. Stud.* 8 (2), 603–608. doi:10.22271/chemi.2020.v8.i2i.8834

Shaikhaldein, H. O., Al-Qurainy, F., Tarroum, M., Khan, S., Nadeem, M., and Salih, A. M. (2022). Phytochemical analysis of maerua oblongifolia, and assessment of the genetic stability of M. Oblongifolia under *in vitro* nanoparticles exposure. *Horticulturae* 8 (7), 610. doi:10.3390/horticulturae8070610

Singh, D., Vignat, J., Lorenzoni, V., Eslahi, M., Ginsburg, O., Lauby-Secretan, B., et al. (2023). Global estimates of incidence and mortality of cervical cancer in 2020: a baseline analysis of the WHO Global Cervical Cancer Elimination Initiative. *Lancet Glob. Heal* 11, e197–e206. Published online December 2022. doi:10.1016/S2214-109X(22)00501-0

Suliman, M. B., and El-hddad, S. (2023). Characterization of chemical constituents of Adansonia digitata L. Using GC- tropical journal of natural product research characterization of chemical constituents of Adansonia digitata L. Using GC-MS. doi:10.26538/tjnpr/v7i6.19

Tadesse, S., Anshabo, A. T., Portman, N., Lim, E., Tilley, W., Caldon, C. E., et al. (2020). Targeting CDK2 in cancer: challenges and opportunities for therapy. *Drug Discov. Today* 25 (2), 406–413. doi:10.1016/j.drudis.2019.12.001

Tao, J., Cui, Y., Duan, Y., Zhang, N., Wang, C., and Zhang, F. (2017). Puerarin attenuates locomotor and cognitive deficits as well as hippocampal neuronal injury through the PI3K/Akt1/GSK-3β signaling pathway in an *in vivo* model of cerebral ischemia. *Oncotarget* 8 (63), 106283–106295. doi:10.18632/oncotarget.22290

Tariq, A., Sadia, S., Pan, K., Ullah, I., Mussarat, S., Sun, F., et al. (2017). A systematic review on ethnomedicines of anti-cancer plants. *Phyther Res.* 31 (2), 202–264. doi:10.1002/ptr.5751

Tatekawa, S., Shimizu, S., Koizumi, M., and Ogawa, K. (2024). Irradiated cell-derived exosomes enhance cell proliferation and radioresistance via the MAPK/erk pathway. *Cancer Genomics Proteomics* 17, 12–17. doi:10.21873/cgp.20425

Vishvakarma, V. K., Yadav, S., Singh, P., and Jain, P. (2023). *In vitro, in silico*, ADME and theoretical analysis of Mn (II) and Co (II) complexes derived from methyl- (Z) - N′-carbamothioylcarbamohydrazonate schiff base ligand. *Chem. Biodivers.* 20 (Ii), 1–8. doi:10.1002/cbdv.202300042

Vordermark, D. (2016). Radiotherapy of cervical cancer. *Oncol. Res. Treat.* 39 (9), 516–520. doi:10.1159/000448902

Wang, Z., Liang, L., Yin, Z., and Lin, J. (2016). Improving chemical similarity ensemble approach in target prediction. *J. Cheminform* 8, 20–10. Published online. doi:10.1186/s13321-016-0130-x

Wavinya Nyamai, D., Musyoki, M. A., Wambua, F., and Matheri, F. (2015). Phytochemical profile of prunus africana stem bark from Kenya pharmacognosy & natural products phytochemical profile of prunus africana stem bark from Kenya. *J. Pharmacogn. Nat. Prod.* 1 (October), 1. doi:10.4172/jpnp.1000110

Xi, C., Shen, J. J., Burston, B., Upadhyay, S., and Zhou, S. (2023). Epidemiological/disease and economic burdens of cervical cancer in 2010–2014: are younger women at risk? *Healthc* 11 (1), 144. doi:10.3390/healthcare11010144

Xia, Y. Z., Ni, K., Guo, C., Zhang, C., Geng, Y. D., Wang, Z. D., et al. (2015). Alopecurone B reverses doxorubicin-resistant human osteosarcoma cell line by

inhibiting P-glycoprotein and NF-kappa B signaling. *Phytomedicine* 22 (3), 344–351. doi:10.1016/j.phymed.2014.12.011

Xing, J., Yi, J., Cai, X., Tang, H., Liu, Z., Zhang, X., et al. (2015). NSun2 promotes cell growth via elevating cyclin-dependent kinase 1 translation. *Mol. Cell Biol.* 35 (23), 4043–4052. doi:10.1128/mcb.00742-15

Yadav, R., Khare, R. K., and Singhal, A. (2017). Qualitative phytochemical screening of some selected medicinal plants of shivpuri district (M.P.). *Int. J. Life-Sciences Sci. Res.* 3 (1), 844–847. doi:10.21276/ijlssr.2017.3.1.16

Yuan, Y. G., Zhang, S., Hwang, J. Y., and Kong, I. K. (2018). Silver nanoparticles potentiates cytotoxicity and apoptotic potential of camptothecin in human cervical cancer cells. *Oxid. Med. Cell Longev.* 2018, 6121328. doi:10.1155/2018/6121328

Zhang, S., Mo, Z., Zhang, S., and Li, X. (2021). A network pharmacology approach to reveal the underlying mechanisms of artemisia annua on the treatment of hepatocellular carcinoma. *Evidence-based Complement. Altern. Med.* 2021, 8947304. doi:10.1155/2021/8947304

Zhao, Y., Li, H., Li, X., Sun, Y., Shao, Y., Zhang, Y., et al. (2022). Network pharmacology-based analysis and experimental *in vitro* validation on the mechanism of Paeonia lactiflora Pall. in the treatment for type I allergy. *BMC Complement. Med. Ther.* 22 (1), 199. doi:10.1186/s12906-022-03677-z

Zhong, S., Zhang, Y., Yin, X., and Di, W. (2019). CDK7 inhibitor suppresses tumor progression through blocking the cell cycle at the G2/M phase and inhibiting transcriptional activity in cervical cancer. *Onco. Targets. Ther.* 12, 2137–2147. Published online. doi:10.2147/OTT.S195655

Zhou, J., Li, H., Wu, B., Zhu, L., Huang, Q., Guo, Z., et al. (2024). Network pharmacology combined with experimental verification to explore the potential mechanism of naringenin in the treatment of cervical cancer. *Sci. Rep.* 14, 1860–1912. Published online. doi:10.1038/s41598-024-52413-9

Zhu, Y., Ren, C., Jiang, D., Yang, L., Chen, Y., Li, F., et al. (2021). RPL34-AS1-induced RPL34 inhibits cervical cancer cell tumorigenesis via the MDM2-P53 pathway. *Cancer Sci.* 112, 1811–1821. doi:10.1111/cas.14874